



UNICA

UNIVERSITÀ
DEGLI STUDI
DI CAGLIARI



Università di Cagliari

UNICA IRIS Institutional Research Information System

This is the Author's manuscript version of the following contribution:

Saba L, Antignani PL, Gupta A, Cau R, Paraskevas KI, Poredos P, Wasserman B, Kamel H, Avgerinos ED, Salgado R, Caobelli F, Aluigi L, Savastano L, Brown M, Hatsukami T, Hussein E, Suri JS, Mansilha A, Wintermark M, Staub D, Montequin JF, Rodriguez RTT, Balu N, Pitha J, Kooi ME, Lal BK, Spence JD, Lanzino G, Marcus HS, Mancini M, Chaturvedi S, Blinc A. International Union of Angiology (IUA) consensus paper on imaging strategies in atherosclerotic carotid artery imaging: From basic strategies to advanced approaches. *Atherosclerosis*. 2022 Aug;354:23-40.

The publisher's version is available at:

<https://doi.org/10.1016/j.atherosclerosis.2022.06.1014>

When citing, please refer to the published version.

International Union of Angiology (IUA) consensus paper on imaging strategies in atherosclerotic carotid artery imaging: from basic strategies to advanced approaches

Abstract

Cardiovascular disease (CVD) is the leading cause of mortality and disability in developed countries. According to WHO, an estimated 17.9 million people died from CVDs in 2019, representing 32% of all global deaths. Of these deaths, 85% were due to major adverse cardiac and cerebral events. Early detection and care for individuals at high risk could save lives, alleviate suffering, and diminish economic burden associated with these diseases.

Carotid artery disease is not only a well-established risk factor for ischemic stroke, contributing to 10%–20% of strokes or transient ischemic attacks (TIAs), but it is also a surrogate marker of generalized atherosclerosis and a predictor of cardiovascular events. In addition to diligent history, physical examination, and laboratory detection of metabolic abnormalities leading to vascular changes, imaging of carotid arteries adds very important information in assessing stroke and overall cardiovascular risk. Spanning from carotid intima-media thickness (IMT) measurements in preclinical stages of atherosclerosis to plaque burden, morphology and biology in more advanced disease, imaging of carotid arteries could help not only in stroke prevention but also in ameliorating cardiovascular events in other territories (e.g. in the coronary arteries).

While ultrasound is the most widely available and affordable imaging methods, computed tomography (CT), magnetic resonance imaging (MRI), positron emission tomography (PET), their combination and other more sophisticated methods have introduced novel concepts in detection of carotid plaque characteristics and risk assessment of stroke and other cardiovascular events.

However, in addition to robust progress in usage of these methods, all of them have limitations which should be taken into account. The main purpose of this consensus document is to discuss pros but also cons in clinical, epidemiological and research use of all these techniques.

Keywords: Carotid artery; atherosclerosis; US; CT; MRI; PET.

a. Current scenario and evidence

I. Targets of carotid imaging

Detailed imaging assessment of extracranial carotid artery disease is critical for appropriate risk stratification and management of those presenting with cerebrovascular ischemia as well as of selected asymptomatic individuals¹.

The degree of luminal stenosis in the carotid bifurcation has historically served as the primary imaging feature for determining ischemic stroke risk and the potential need for surgery.

Contemporary multimodality imaging including ultrasound, magnetic resonance imaging (MRI/MRA), CT angiography (CTA) and even positron emission tomography (PET-CT) or PET-MRI methods target more detailed visualization of carotid plaque components that indicate plaque vulnerability (e.g. maximum plaque thickness and volume, calcification, ulceration, intraplaque hemorrhage, inflammation, intraplaque neovascularization, lipid-rich necrotic core, and thin or ruptured fibrous cap)¹ (**Table 1**).

Not infrequently a carotid scan can indirectly (through flow patterns) detect the status of other vascular territories or even other abnormal findings of surrounding structures (e.g. a thyroid nodule)².

II. The role of carotid arteries imaging:

There are several reasons that require carotid imaging, the predominant being evaluation after a cerebrovascular event but also for CVD screening, risk stratification and prevention as well as for surveillance after a carotid procedure^{1,3}.

Imaging of the carotid bifurcation is essential in all patients with symptoms of cerebral ischemia, whether they present as a TIA or complete stroke^{1,3}. If significant carotid artery disease is identified as the source of symptoms, these patients are candidates for a carotid intervention to prevent a secondary stroke³. Although imaging for this indication is most often performed with a carotid duplex ultrasound, when evaluation of the vessels proximal or distal to the cervical portion of carotid artery is required for diagnosis or to plan endovascular or surgical therapy, additional imaging with CTA, MRA or digital subtraction angiography (DSA) is indicated³.

The use of imaging methods for screening for carotid artery disease in the general population, in particular to identify significant disease that will prompt an intervention to prevent a stroke are controversial³. However, targeting selected groups of neurologically asymptomatic patients is well established. These groups can be high-risk patients aged >55 years with cardiovascular risk factors, patients with a carotid bruit on clinical exam, Hollenhorst plaque on fundoscopic examination, silent infarction on brain imaging examinations³.

Finally, surveillance after a carotid intervention is common practice established on the natural history of ipsilateral restenosis, contralateral disease progression and associated stroke risk.

b. Ultrasound

I. Stenosis

Grading and stratification of carotid stenosis is mainly based on multiparametric, hemodynamic criteria on Duplex ultrasound⁴ (**Table 2**). The most important parameters are the measurement of the peak systolic and the end-diastolic flow velocity within the stenosis. The accuracy of Duplex ultrasound compared with angiography for detecting >50% and \geq 70% stenosis, respectively, is very good, with a positive predictive value of >90% and a specificity of >85%⁵. Duplex ultrasound is

recommended as the primary imaging modality to assess the extent and severity of extracranial carotid stenosis⁶. Various studies have also shown that the risk of cerebrovascular events increases not only with the severity of the stenosis but also with rapid progression of the degree of stenosis^{7,8}. Therefore, patients with an asymptomatic carotid stenosis (ACS) undergo usually annual ultrasound monitoring.

II. Features of vulnerability

Duplex ultrasound can assess not only the degree of stenosis,^{4,9} but also several sonomorphological characteristics which are associated with plaque vulnerability¹⁰. Hypoechogenicity including a low grey scale median (GSM)^{11,12}, large juxtaluminal hypoechogenic area¹³, heterogeneous echotexture^{14,15}, or higher plaque burden (plaque area, total plaque area [TPA], or plaque volume)^{16,17}, surface irregularities and ulceration¹⁴ on B-mode ultrasound are sonographic features of plaque vulnerability with increased embolic risk⁶ (**Table 2**).

A 2020 review article summarized many of the advantages of measuring carotid plaque burden, which is far superior to measuring carotid IMT in many ways¹⁶.

Carotid plaque burden (CPB) is useful for risk stratification, treatment of atherosclerosis, research into the biology and genetics of atherosclerosis, and evaluation of new therapies against atherosclerosis.

Measured as TPA or as 3D plaque volume, CPB is highly correlated with coronary calcium¹⁷, and as predictive of events¹⁸; while IMT is neither^{17,18}. A recent study reported that CPB was superior to coronary calcium for risk stratification in women¹⁹; it is also detected at a younger age. CPB also has significant advantages compared with coronary calcium, because it can be measured repeatedly, to assess and adjust the effects of therapy. Serial assessment of plaque burden in conjunction with life-style and pharmacological treatment according to guidelines, called “Treating Arteries” (instead of merely treating risk factors), markedly improves therapy for atherosclerosis. In

part this is because showing patients images of their plaque markedly improves compliance with lifestyle changes and medication²⁰. Among high-risk patients with asymptomatic carotid stenosis, implementation of “Treating Arteries” was associated with a >80% reduction of the 2-year risk of stroke/myocardial infarction/vascular death²¹. In prevention clinics across Argentina, “Treating Arteries” was implemented in 2010; among patients age >65, the annual risk of cardiovascular events declined from 5.85% to 2.35% between 2011 and 2015²². Patients in Germany who were treated with lipid-lowering drugs on the basis of a high CPB had a much lower risk of cardiovascular events over 3.9 years, than patients treated only on the basis of serum cholesterol: (5.4% vs 23%, respectively)²³. It has been supported that “Treating arteries” without measuring plaque would be like treating hypertension without measuring blood pressure.”²⁴

Studies using CPB identify new causes of atherosclerosis, either through genetic studies²⁵, or studies of new risk factors such as toxic metabolites produced by the intestinal microbiome²⁶. Such studies will lead to new therapies for atherosclerosis, and measurement of CPB markedly reduces sample size and duration of studies to evaluate such new therapies²⁷.

New automated methods based on machine learning for measuring TPA for measuring TPA, 3D carotid plaque burden²⁸ and Vessel Wall Volume²⁹ (which can be measured in persons without plaque, so it can replace IMT) will make it much easier to implement this. These new methods are very fast, reliable, and reproducible³⁰. **Figure 1** shows comparisons of automated with manual segmentation.

III. Transcranial Doppler Detection of Embolic Signals in Carotid Artery Disease

Transcranial Doppler ultrasound (TCD) is a non-invasive technique that can be used to detect circulating emboli/intracranial embolism. These emboli appear as short duration, high-intensity embolic signals/intracranial embolism and are accompanied by a characteristic chirping sound. TCD circulating emboli detection has been shown to have a high sensitivity and specificity in

experimental studies³¹, although in clinical practice care needs to be applied in distinguishing true embolic signals (also known as high intensity transient signals) from artefact. Consensus criteria have been developed to allow this³².

Studies have demonstrated that large artery stroke is the subtype associated with highest prevalence of embolic signals, compared with cardioembolic and lacunar stroke³³. In patients with recently symptomatic carotid stenosis (SCS), during a 1-hour recording from the ipsilateral middle cerebral artery (MCA) embolic signals can be identified in about 40% of individuals³⁴. A higher prevalence has been reported in patients with more recent symptoms, SCS compared with ACS, and plaque imaging characteristics indicating higher risk plaque³⁵. Prospective longitudinal studies have demonstrated that embolic signal detection predicts future stroke risk in both SCS³⁴ and ACS^{36–38,39,40}. The effect is additive to that obtained by plaque imaging modalities such as carotid ultrasound⁴¹. It has been suggested that embolic signal detection may be a useful method to identify ACS patients at high risk who may particularly benefit from carotid endarterectomy (CEA)³⁹ although this needs to be proven in a randomized intervention study. Conversely, patients with an absence of embolic signals may do well with intensive medical management alone.

Embolic signal detection has been used to evaluate the effectiveness of antithrombotic drugs in carotid artery disease³⁸. Studies have shown that aspirin, clopidogrel but also statins reduces embolic signals^{42,38,43}. Combination antiplatelet regimens such as aspirin and clopidogrel were more effective than aspirin alone in randomized controlled trials^{38,44}. This paralleled subsequent studies demonstrating their greater effectiveness in preventing recurrent stroke after minor stroke and TIA^{42,44}, and reinforcing the evidence that embolic signal detections may be a useful surrogate marker to identify efficacy of antithrombotic agents.

IV. Impact of contrast material

As a complement to conventional duplex ultrasound, intravenous application of ultrasound contrast agents has greatly enriched sonographic imaging in vascular medicine^{45,46}. Contrast agents consist of small microbubbles, which circulate strictly intravascularly in the bloodstream for several minutes after application. Due to their non-linear reflection pattern, a contrast-specific ultrasound image is obtained, which enhance not only the vessel lumen, but also the microcirculation in the vessel wall (vasa vasorum) including intraplaque neovascularization (IPN)⁴⁷.

In the carotid artery, contrast-enhanced ultrasound (CEUS) is helpful in distinguishing complete vessel occlusion from very high-grade carotid stenosis. In addition, particularly hypoechogenic plaques can be well detected and surface irregularities and ulcerations of arteriosclerotic lesions can better delineated⁴⁸⁻⁵⁰. The most important value of CEUS lies in the detection and quantification of IPN⁴⁶, which is usually performed semiquantitatively^{51,52}. Such visual based quantification has good intra- and interobserver variability, but a more objective, purely quantitative measurement of IPN ranging from measurements of maximal contrast enhancement to automated, computer-assisted quantification of relative perfused area is desirable^{53,54, 55}.

IPN on CEUS has been compared with the corresponding vascularization on histopathologic examination in patients with carotid stenosis before CEA showing a good correlation between the IPN and the extent of microvessels and inflammation within the plaque on histology^{56,57, 58}.

It has been demonstrated that hypoechogenic plaques, which were considered vulnerable on B-mode ultrasound, had higher IPN on CEUS than the more stable hyperechogenic lesions^{51,56}.

Various retrospective studies of patients with carotid plaque revealed that those lesions with a higher embolic risk had increased plaque IPN on CEUS imaging. Thus, it was shown in a meta-analysis that the prevalence of IPN was higher in SCS compared with ACS patients¹⁵ and correlates with cardiovascular events⁵⁹. Different prospective studies also demonstrated that in patients with recent ischemic cerebrovascular event the risk of future ischemic stroke or TIA was significantly

associated with IPN in carotid CEUS examination^{60,61}. IPN on CEUS imaging was also found to be predictive of significant and complex coronary artery disease and future cardiovascular events⁶². Carotid CEUS examination has the potential to improve risk stratification with respect to the occurrence of embolization by grading IPN in patients with carotid plaque and stenosis. This could be useful to monitor therapeutic interventions⁶³ and to better select patients with carotid stenosis, who benefit from a possible invasive therapy⁴⁷.

B. Computed tomography

I. Stenosis

CTA has evolved along with the technologic advances of CT hardware and software. Modern CTA, performed with multidetector high-speed CT hardware and evaluated with 3D reformatting software, accurately and reliably depicts carotid disease and allows for direct quantification of carotid stenosis in millimeters⁶⁴⁻⁷⁰.

CTA is an anatomic study of arteries, allowing for direct evaluation of carotid stenosis. CTA is fast, with images of the head and neck acquired over approximately 5-15 seconds during contrast injection. 512 × 512 memory matrix multidetector CT scanners allow acquisitions with near-isotropic spatial resolution and an effective section thickness as small as 0.5 mm⁷¹. For evaluation of carotid arteries and the cerebral vasculature, it is possible to narrow the nominal section thickness to obtain a submillimetric dataset. This ability, combined with 3D image rendering, provides an excellent accuracy for the measurement of the degree of stenosis⁷¹. In light of the relative benefits of CTA in reference to safety, time, and related lower cost than DSA, it is compelling to use CTA when the indication for angiography is not to deliver a therapeutic intervention such as stenting, but

to accurately characterize the degree of stenosis. Venous filling is not an artefact for neck carotid imaging, because arteries are easily recognized as distinct from veins.

CTA evaluation is mainly based on axial sections and curved planar reformations (CPR). CTA has been shown to have a pooled sensitivity of 95% and specificity of 98% for the detection of >70% stenoses⁷². There are advantages of quantifying carotid stenosis by direct millimeter measurements instead of or in addition to the well-known North American Symptomatic Carotid Endarterectomy Trial (NASCET)–style ratio calculations⁷³. Multi-slice CTA can in addition detect tandem stenoses in the region of the carotid origin from the aorta, the carotid siphon, and the intracranial portion of the carotids. CT is able to provide a comprehensive evaluation of patients with acute stroke by using a combined approach of pre-contrast CT to detect hemorrhage and manifest infarction, perfusion CT measurements to differentiate between penumbra and infarct and CTA to detect the occluded vessel as well as potential concomitant carotid abnormalities.

II. Features of vulnerability

Atherosclerotic disease is a complex, heterogeneous, and multifactorial condition with several type of components in the same plaque. The role of plaque imaging is to identify those imaging biomarker features of carotid plaque that are related to vulnerable plaque^{74,75,76,77}. In particular, CTA thanks to its spatial resolution is able to assess the carotid artery lumen and the arterial wall. A key feature of vulnerable carotid plaque is Intraplaque haemorrhage (IPH), that is defined by the accumulation of blood components within the carotid plaque⁷⁸. Regarding the pathogenesis of IPH, most of the authors suggest that it is linked to the rupture of neovessels or plaque rupture itself, and some trigger events including inflammation, metabolic diseases or diabetes may precipitate this condition⁷⁸. IPH represents the strongest imaging feature associated with the occurrence of stroke⁷⁹, and it is also more common in carotid artery ipsilateral to embolic stroke of undetermined

source⁸⁰. Conflicting results have been reported about the role of CT to detect this feature.

However, studies suggest that CTA is able to discriminate the presence of IPH, both directly according to attenuation at 25 HU⁸¹ and indirectly with the presence of calcified rim and soft internal plaque⁸².

The thin fibrous cap with a lipid-rich necrotic core (LRNC) represents one of the most important features of the carotid artery vulnerable plaque model. In particular, LRNC is considered collection of heterogeneous tissue composed of cholesterol crystals and necrotic debris of apoptotic cells⁸³.

The fibrous cap is a layer of fibrous connective tissue that contains macrophages and smooth-muscle cells, and particularly the morphology and thickness of the fibrous cap are indicative of rupture⁸⁴. These two imaging features are associated with the risk of stroke, especially when a thin fibrous cap cover a large LRNC⁸⁵.

In addition, the LRNC size correlates with future ipsilateral carotid symptoms⁸⁶. CT can be used to visualize lipid components of the LRNC, thanks to lipid tissue attenuation properties, but may more hardly discriminate between LRNC and IPH, given the attenuation values of these two features⁸⁶.

Similarly, the evaluation of the fibrous cap with CT is not considered optimal because of the artefact related to halo-effect and edge-blur⁸⁷.

Another feature of plaque vulnerability is inflammation of the carotid artery plaque. Different type of inflammatory cells have been identified in the carotid plaque usually located in the plaque shoulder, cap or both with a role in plaque “instability”^{87,88}. Beyond the presence of macrophages, plasma cells are also associated with the risk of rupture and the occurrence of cardiovascular events⁸⁸.

Similarly, plaque neovascularization is considered a marker of plaque vulnerability, which is related to newly formed neovessel arising into the intima and is associated with plaque activity⁸⁶.

The presence of neovascularization in carotid plaque represents an elements of instability because these microvessels are prone to rupture due to its immature and imperfect endothelial structure⁸⁹.

CTA can identify the presence and the degree of neovascularization thank to its ability to detect contrast plaque enhancement ⁹⁰.

Beyond plaque composition, vulnerable plaques tend to be associated with plaque surface morphology (i.e. smooth, irregular, or ulcerated) ⁷⁵. In particular, the presence of ulceration, defined as an intimal defect larger than 1 mm in width ⁸⁶, is considered a risk feature for cardiovascular events ⁹¹. The carotid plaque surface morphology can be better assessed with CTA in comparison with other non-invasive imaging modalities, as demonstrated by Saba et al ^{92,93}.

Also, carotid plaque volume is a crucial determinant of plaque vulnerability. Rozie et al. demonstrated that plaque volume and the relative subcomponents of the plaque are associated with plaque vulnerability and stroke ⁹⁴. Thanks to its excellent spatial resolution, CTA can easily evaluate this parameter ⁷⁴.

Among the multiple parameters that have been indicated as responsible for an increased vulnerability, conflicting results have emerged in the identification of a role for calcium. Emerging research has suggested various mechanisms in calcium deposition leading to different phenotypes of carotid plaque calcification ^{95-97,98,99}. Yang et al. investigated the association between calcium configurations and ulceration with IPH, demonstrating that superficial, multiple, and thin calcifications were associated with IPH. The authors concluded that the size and location may represent a marker of high-risk plaque ⁹⁶. **Table 3** summarizes the CT features of plaque vulnerability and its strengths and limitations.

III. Ancillary findings in carotid imaging

While evaluation of vessel patency and plaque characteristics remains the main reason to perform CT/MR-imaging of the carotid arteries, a variety of ancillary findings can be encountered (**Table 4**). Some are merely incidental findings with no further clinical relevance, while others represent a

different etiology of the patient's complaints with clear implications for further treatment and prognosis. Although a detailed scope of all possible ancillary findings is outside the scope of this paper, some important entities will now further be discussed.

Carotid dissection

As in the aorta, a dissection of the carotid artery wall constitutes a disruption of the carotid intima layer, with blood flowing into the vessel wall and the creation of a true and false lumen¹⁰⁰.

A carotid artery dissection can be spontaneous or post-traumatic¹⁰⁰. When spontaneous, an underlying condition must be ruled-out, which can include entities like fibromuscular dysplasia, Marfan syndrome and Ehler-Danlos syndrome^{100,101}. It is important to scrutinize the other cervical arteries as well, as they may exhibit morphological changes contributing to a correct diagnosis (e.g. signs of fibromuscular dysplasia in the contralateral artery)¹⁰².

The pathophysiology of a carotid dissection explains its imaging findings¹⁰¹. In contrast to the aorta, the dissection flap is seldom seen in a carotid artery dissection, as the false lumen usually thromboses and creates a semicircular non-enhancing soft tissue density surrounding the true lumen (**Figure 2**)¹⁰¹. This makes MR-imaging especially useful, as this thrombus will lead to a hyperintense signal on fat-suppressed T1-weighted images due to blood breakdown products. It can be problem-solving in cases in which the presence and extend of the dissection can be difficult to assess on CT alone, as the difference in contrast between the wall hematoma and surrounding tissues can be limited¹⁰¹.

A carotid dissection usually appears in the supra-bulbar internal carotid artery. In many cases it will remain limited to the extracranial segment, but extension into the skull base can occur^{101,102}.

Carotid web & thrombus

A carotid web is identified as a small, (curvi)linear soft tissue density protruding into the carotid lumen usually at the level of the carotid bulb^{103,104}. According to some authors it represents a

variant of fibromuscular dysplasia, and is associated with an increased risk for stroke, especially in younger patients without classic vascular risk factors¹⁰⁵.

A thrombus presents as a non-enhancing central structure surrounded by flowing blood (so-called “donut” sign). While rare, its presence is important as it is associated with an increased risk for stroke, but also to conditions leading to a hypercoagulable state like malignancy, infections and pregnancy^{103,104}.

Inflammatory & infectious conditions

Carotid vasculitis can be defined as the inflammation of carotid artery walls with or without necrosis, leading to stenosis or occlusion of the lumen¹⁰⁶. Vasculitis may be associated with systemic connective tissue disorders or may be secondary to infection, malignancy, drugs, or radiation therapy¹⁰⁶. For a correct diagnosis, relevant laboratory tests are also required. The 2012 Chapel Hill Consensus Conference defined different types of vasculitis in terms of (a) the size of the involved arteries and (b) associated pathologic lesions¹⁰⁷. The most frequent vasculitis involving carotid arteries are Takayasu arteritis and Giant cell arteritis^{106,107}. Infectious extracranial carotid disease rare and usually caused by *Staphylococcus aureus*, *Salmonella*, and streptococcus species. When present, it can manifest as an infected aneurysm with focal weakening of the wall, development of a pseudo-aneurysm and increased rupture risk (**Figure 2**).

With CTA / MRA imaging, signs of carotid vasculitis are vessel wall thickening (mostly concentric representing a key parameter in the differential diagnosis) and contrast enhancement. Usually there is no preference for involvement of the carotid bifurcation (different to atherosclerotic disease). In case of active vasculitis contrast enhancement of the thickened vessel wall may be seen on both CT and MR¹⁰⁶.

Other

Any other condition or anomaly that is encountered during a carotid examination must be reported. These include rare instances like carotid body tumours or any other condition that influences clinical management.

C. Magnetic Resonance Imaging

I. Stroke Risk Assessment and Characterization of Low-Grade Carotid Atherosclerosis

Risk assessment of carotid atherosclerotic plaque for cerebrovascular ischemic events has historically relied on angiographic measures of stenosis, with thresholds for revascularization defined by randomized clinical trials that date back to the early 1990's^{91,108,109}. The established threshold for SCS is 70%, although revascularization is often considered for stenosis beginning at 50% when symptomatic and 60% when asymptomatic^{91,108,110,111}. Stenosis has worked well in these studies considering it is a surrogate for plaque burden, which is strongly associated with ischemic stroke risk¹⁶. However, there have been substantial technical advances in our ability to identify features of atherosclerotic plaque that can improve our precision for stratifying risk¹¹²⁻¹¹⁴. This is especially important for atherosclerotic plaques that fall under the thresholds for angiographic detection of risk. Risk estimation for stroke from a plaque causing less than 50% stenosis must be a priority considering the high prevalence of low-grade carotid stenosis in the community¹¹⁴. For example, in the Cardiovascular Health Study detectable carotid stenosis was present in 62% of women and 75% of men aged ≥ 65 years, with only 7% of men and 5% of women having stenosis $\geq 50\%$ ¹¹⁵. Risk analysis of carotid plaque must also consider the accommodation of atherosclerotic plaque formation by flow-mediated outward remodeling regulated by endothelial cells to preserve lumen caliber. This endothelial response is overcome once plaque size reaches a threshold and angiographic stenosis becomes detectable. For example,

there is evidence that angiographic narrowing of the extracranial internal carotid artery is not detected until plaque burden reaches 61.9%¹¹⁶ or 63.1%¹¹⁷ area stenosis measured on black blood MRI exams, highlighting the large burden of plaque that can exist in low-grade carotid atherosclerosis.

II. High-Risk Carotid Plaque Features Detectable on MRI

Based on histopathologic validation studies¹¹⁸, MRI has been shown to have high accuracy in detecting key high-risk carotid plaque features. For example, using a multi-sequence protocol with a carotid coil, MRI can identify the presence of a LRNC, thinning/rupture of the fibrous cap, ulceration, and IPH, all of which are strong predictors of future stroke risk¹¹². Although the literature strongly supports a potential role for multi-contrast, multi-sequence MRI to aid in risk stratification before stroke and identify culprit lesions after stroke, adoption of these techniques has been limited in the context of acute stroke imaging due to exam length, need for dedicated coil hardware and/or gadolinium, and complexity in image interpretation¹¹⁹.

In recent years, converging evidence has identified the use of a single T1-weighted, fat-suppressed sequence to identify IPH as a particularly valuable imaging strategy to incorporate into clinical practice¹²⁰. This sequence includes an inversion pulse to suppress the blood in the lumen. In such an approach, IPH can be identified by the presence of T1-hyperintense signal within carotid plaque when noted to be brighter than the signal intensity of adjacent background skeletal muscle^{121,122}. A recent meta-analysis of individual patient data of 560 patients from 7 cohort studies showed the annualized rate of ipsilateral stroke in those with carotid IPH to be markedly increased compared to those without IPH across all stenosis severity levels, including those with <50% stenosis¹²³. For this reason, MRI based IPH identification has significant promise not only in identifying patients who may benefit the most from surgical revascularization procedures, but also in identifying culprit low-grade plaques responsible for ischemic strokes which would otherwise be characterized as

cryptogenic in nature^{124,125}. Patients with an absence of IPH may do well with intensive medical management alone. Given the promise of carotid IPH as a clinically useful MRI risk marker, randomized stroke prevention trials using IPH as a selection criterion will be needed to establish whether there is evidence to support the widespread adoption of this approach in clinical treatment decision-making.

III.Role of MRI in Assessment of Intracranial Carotid and Aortic Arch Atherosclerosis

MRI technology has been shown to have an increasing clinical role in the evaluation of atherosclerotic plaques in locations other than the extracranial carotid artery. MRA has high sensitivity and specificity for identification of stenoses >50% involving the intracranial ICA^{126,127} and the MCA¹²⁸. It is routinely utilized in clinical practice to identify patients suspected of harboring intracranial stenosis. Limitations of intracranial MRA include long acquisition times and overestimation of the degree of stenosis because of flow artefact.

A major advantage of MRI sequences in the assessment of intracranial plaques is the concomitant acquisition with parenchymal brain imaging. Recent MRI techniques also allow to further characterize plaque composition and its hemodynamic effects. High resolution vessel wall MRA provides further characterization of the intracranial arterial wall and pathology by suppressing signal from intravascular blood. It is increasingly used to differentiate among different causes of intracranial steno-occlusive disease and to identify/characterize plaques causing minimal or no narrowing on luminal imaging in patients with otherwise unexplained ipsilateral stroke^{129, 130-132}. The hemodynamic effects of intracranial plaques can be measured with quantitative MRA which combines traditional MRA-Time-of-Flight (TOF) and contrast-enhanced (CE)-MRA. This technique allows quantification of the hemodynamic significance of a plaque, which may not necessarily correlate with degree of narrowing¹³³.

Aortic arch atheroma has been recognized as a potential cause of emboli in patients with cryptogenic stroke and MRI-based multicontrast plaque imaging was used to recognize vulnerable

aortic arch plaques¹³⁴. The addition of 4D flow measurements identifies potential embolization pathways to the brain and is especially useful to suggest possible retrograde embolization in patients with vulnerable plaques located in the proximal descending aorta immediately distal to the origin of the large extracranial arteries¹³⁴.

D. Other techniques

I. PET

PET enables molecular imaging of biological and biochemical processes in vivo, whereas hybrid PET/CT¹³⁵ or PET/MRI^{136,137} also provides additional information on plaque morphology. The glucose analogue 18F-Fluorodeoxyglucose (FDG) is taken up by cells with a high metabolic rate, such as macrophages within an atherosclerotic plaque, and therefore enables to quantify the inflammatory activity within carotid atherosclerotic plaques¹³⁸. In order to correct for uptake of the tracer in the blood pool, it is recommended to use the target to background ratio (TBR) to quantify FDG uptake¹³⁹. TBRmax is defined as the ratio of the maximal standardised uptake value (SUVmax) measured in the plaque and the mean SUV (SUVmean) in the blood pool¹³⁹. In a study of 49 patients that underwent an 18F-FDG PET examination before CEA, it was shown that the TBRmax correlates with the extent of CD68 staining, a measure for macrophage content of the plaque ($r=0.51$, $P<0001$) (**Figure 3**)¹⁴⁰. Various studies demonstrated higher uptake in symptomatic compared to asymptomatic plaques, while the activity in symptomatic plaques decreases in the months after the event^{140,141,142,143,144}. Moreover several studies reported weak correlations between 18F-FDG uptake on PET and CT/MRI parameters of carotid plaque (Spearman ρ : 0.098-0.39), indicating that PET may have additive information for risk assessment^{141,145,146}. Importantly, 18F-FDG uptake was demonstrated to predict early post-PET stroke recurrence with a fully adjusted hazard ratio of 4.57 (95% confidence interval [CI], 1.5–13.96; $p=0.008$) in a pooled cohort of 196 patients with carotid stenosis and recent stroke/transient ischemic attack with 8 post-PET stroke

recurrences. Although most extensively validated, a disadvantage of ^{18}F -FDG is that the tracer is not specific. Recently, more specific tracers for plaque inflammation have been proposed^{147–149}, but these still need to be validated in larger studies. Alternatively, uptake of ^{18}F -sodium fluoride (NaF), a marker for active microcalcific processes, was reported at the site of carotid plaque rupture and larger uptake was demonstrated in symptomatic plaques^{140,150,151}. The value of ^{18}F -NaF for risk stratification is currently under investigation in an ongoing prospective multicenter trial (PREFFIR; unique identifier: NCT02278211).

II. Intravascular Imaging Platforms

The use of intravascular technologies for intraluminal imaging of carotid atherosclerosis is currently limited to highly selected cases and includes fiber-bundle angioscopy (FBA), IVUS and optical coherence tomography (OCT). FBA was introduced in the early 1980s and initially applied to assess plaque disruption, luminal thrombus and stent placement^{152,153}. Despite the initial enthusiasm given the unprecedented images of the arterial lumen and surface, the poor image quality (<10,000 pixels even with FBA), the large size and the excessive stiffness of the cameras significantly limited adoption¹⁵⁴. Recent advances in photonics and optics allowed the development of Scanning Fiber Angioscopy, a miniature laser-based platform capable of generating high resolution ($\sim 12\ \mu\text{m}$, or >250,000 pixels) structural, biochemical and biological vascular videos in real time (**Fig 4A**)^{154,155}. IVUS was introduced in the late 1980s and employs an intravascular piezoelectric transducer that creates waves that propagate through blood and tissue. IVUS generates cross sectional imaging without the need of clearing the intravascular blood, but the resolution is poor (100–150 μm). IVUS has been clinically used to characterize the structure of carotid plaques by virtual histology, measure the degree of stenosis, and evaluate stent apposition and plaque protrusion in CAS (**Fig 4B**)^{156–158}. OCT shines a near-infrared laser sideways and a small portion of this light (scattering) that reflects from sub-surface tissues is collected and processed by

interferometry. Automated pullback in a bloodless lumen result in cross-sectional images of arteries. The use of OCT in carotid arteries continues to be very limited in the evaluation of disrupted plaques, stent apposition and tissue prolapse in CAS^{159,160}.

E. A look into the future

I. Artificial intelligence

As stroke is the second leading cause of global mortality, this demonstrated the need for improved tools in the management of occlusive vascular disease^{161,162}. Patients with cardiovascular disease leading to stroke often require significant medical imaging in the acute, sub-acute, and chronic settings, using a range of imaging modalities. Vascular imaging is then used as a key source of information in the determination of appropriate clinical management. In the era of modern medicine, AI is an evolving field which is experiencing a steady development in vascular imaging^{77,163,163,164}. In daily clinical practice, plaque assessment is performed through manual measurement of the degree of the stenosis and visual evaluation of plaque composition^{6,165}. However, a manual evaluation has various limitation, including long analysis time and being highly dependent on the operator. AI may evaluate carotid plaques with their vulnerable features to decide whether invasive investigation and treatment are necessary.

US is the modality of choice for initial evaluation and confirmation of carotid artery disease: characteristics of the carotid plaque in patients with carotid stenosis can identify those patients with relatively higher risk for stroke and help select patients who may benefit from intervention over medical treatment alone or vice versa. Symptomatic plaques tend to produce more tight stenosis, be more hypoechoic, have a large juxtaluminal black area close to the lumen without a visible echogenic cap, and discrete white hyperechoic areas compared with asymptomatic plaques^{166,167}. Additional and more precise information can be derived from software implementations applied to

ultrasound: 3D/4D, Intravascular Ultrasound (IVUS), CEUS, Sonoelastography, Vector Doppler, Grayscale Median (GSM), Radiofrequency etc. The large datasets obtained from all these imaging sources are traditionally interpreted qualitatively by clinicians but are highly heterogeneous, varying due to differences in patient, imaging technology, and site scanning protocols. Current measurement methods are time-consuming and do not utilize the power of knowledge-based paradigms such as artificial intelligence (AI), a branch of computer science that includes machine learning (ML), deep learning (DL) and convolutional neural networks (CNNs) (**Figure 5**). AI excels at automatically recognizing complex patterns and providing quantitative assessment for imaging data, showing high potential to assist physicians in acquiring more accurate and reproducible results^{168,169}. Recently, a DL-based model was applied for carotid IMT and lumen measurement¹⁷⁰. It was the first artificial intelligence-based approach in ultrasound-based carotid artery segmentation and carotid IMT (cWT þ CP) measurement that used 13 layers of convolution layers for feature extraction and three up-sample layers for segmentation. Deep learning resulted in a useful tool for carotid ultrasound-based characterization and classification of symptomatic and asymptomatic plaques in a more recent paper¹⁷¹ where implementation with a supercomputer configuration was more precise and faster if compared with other AI systems. Further and more accurate measurements can be obtained when an AI-based model utilizing DL methodology is used on image patches rather than full-size images, mainly to have better local control in small regions rather than the whole image at once^{168,170,172}. A new method consisting in a novel design of 10 types of solo deep learning (SDL) and hybrid deep learning (HDL) models focused on automated plaque segmentation in the internal carotid artery (ICA) has shown to be very useful in identifying plaques at risk of rupture: the system is very fast and precise (it takes <1 s per image) and it may therefore be practical to introduce such an AI-based system to detect rupture-prone plaques (or vulnerable plaque detection)¹⁷³.

In addition to the improved ability to define so-called vulnerable plaques to enable the best therapeutic approach, AI has also proved to be useful for the evaluation of carotid artery stenting

(CAS) prognosis and in prediction of persistent hemodynamic depression after carotid angioplasty^{174,175}. Of note, the application of AI to ultrasonographic diagnostics for better diagnosis and possibly new classification and standardization methods¹⁷⁶ requires a close collaboration among computer scientists, clinical investigators, clinicians, and other users in order to identify the most relevant problems to be solved and the best approach and data sources to achieve this.

An AI-based approach has also proven its usefulness in CT. Acharya et al investigated a supervised-learning model to classify carotid artery image into symptomatic and asymptomatic using a combination of local binary model and wavelet energy features¹⁷⁷. The authors reported sensitivities, specificities, and accuracies of 0.88, 0.865, and 0.902, respectively¹⁷⁷. Dos Santos et al. proposed a fully-automated, user-independent tool for the segmentation and analysis of atherosclerosis in the extracranial carotid arteries, reporting a performance of 83% with accuracy, sensitivity, and specificity values of 71 %, 83 %, and 25 %, respectively with an average difference between manual and automated analysis of 37 % (p = 0.27) and an average analysis time of 1381 s per patient¹⁷⁸. AI models have been also developed to simplify plaque characterization and predict histological plaque composition. Hanning et al. tested a ML-based analysis of admission non-contrast CT and CTA to predict thrombus composition with its fractions of fibrin and red blood cells¹⁷⁹. This analysis included 112 patients who underwent thrombectomy due to a carotid or middle cerebral artery occlusion, evaluating both vessel walls, thrombi and peri-vascular tissue response. The ML based algorithm demonstrated an AUC of 0.83 for differentiating thrombi with a high fraction of red blood cells (sensitivity and specificity of 77% and 74%, respectively) and an AUC of 0.84 for differentiating fibrin-rich thrombi (sensitivity and specificity of 81% and 73%, respectively)¹⁷⁹. Another research investigated the ability of a DL-based model to identify symptomatic patients from asymptomatic patients and further discriminating between culprit and non-culprit carotid arteries in symptomatic patients¹⁸⁰. This proposed model was 92% accurate in differentiating between symptomatic and asymptomatic patients, and 71% accurate in discriminating between culprit versus non-culprit carotid arteries in symptomatic patients¹⁸⁰. The

relationship between carotid vessel image parameters and stroke risk was also investigated by Lal et al. using an artificial intelligence algorithm for risk stratification in carotid atherosclerosis incorporating a combination of carotid plaque geometry, plaque composition, patient demographics and clinical information¹⁸¹ AI is able to mesh a large amount of quantitative imaging data to clinical parameters, that may be a new frontier of AI in carotid plaque risk assessment improving diagnosis and decision-making in daily clinical practice.

AI is transforming most healthcare domains including carotid MRI. AI is increasingly used to reduce manual effort in carotid MRI measurements. Using a convolutional neural network (CNN) based algorithm called DeepMAD to separately segment the carotid lumen and outerwall contours on 2D T1w turbo spin echo MRI, Wu et al identified slices with atherosclerotic plaque¹⁸². Similarly, Samber et al used two separate CNNs for lumen and outerwall segmentation of 2D T2w turbo spin echo MRI¹⁸³. Chen et al demonstrated a CNN algorithm called LATTE for segmentation¹⁸⁴ of the carotid vessel wall on 3D-MERGE¹⁸⁵ black-blood MRI using a polar transformation centered on the carotid after vessel identification. To make the segmentation robust to inter-scanner differences, domain adaptation for LATTE was developed and shown to improve the identification of advanced plaque¹⁸⁶. Thus, quick, and automated screening for carotid plaque using 3D-MERGE is made possible by LATTE. The next frontier for carotid AI applications lies in plaque component segmentation. CNN based segmentation of plaque components such as lipid-core, calcification, and intra-plaque hemorrhage on multi-contrast 2D MRI is able to better match the human expert's plaque component segmentation than non-CNN methods¹⁸⁷. Zhang et al compared several ML methods¹⁸⁸ for plaque component segmentation using a specific sequence called SNAP¹⁸⁹. However, these methods are 2D MRI based and need to be modified for use with 3D carotid MRI. With future development, multi-contrast 3D plaque component segmentation may allow complete carotid plaque analysis and quantification with minimal user intervention thereby reducing clinician workloads and expand the applications of carotid plaque MRI.

CNNs have also found application in carotid MRA. Koktzoglou et al demonstrated that non-contrast carotid MRI can be accelerated to below three minutes when combined with a denoising of MRA using CNNs¹⁹⁰. Ziegler et al used the DeepMedic CNN on CE-MRA to segment the carotid artery into common, internal and external carotid segments¹⁹¹.

Information contained in the gray-scale differences among tissues are easily summarized by human derived features. Radiomics can extract traditional gray scale level features from images to improve the diagnostic capabilities of carotid MRI. Zhang et al showed that adding radiomic features of carotid plaque to traditional plaque features improved the model's ability to predict symptom status¹⁸⁸. Application of such radiomics specific to the carotids requires segmentation of the carotid lumen and outer wall. Hence future combination of CNN based segmentation methods combined with radiomics may enable a comprehensive and automated analysis of both carotid MRI and other clinical variables to predict patient outcomes.

II. Radiomics

Since the 1990s, the improvement of resolution, which allows the identification of increasingly smaller lesions, and the availability of imaging modalities that provide morphological and functional information have introduced new scenarios and new diagnostic possibilities. The introduction of new imaging technologies as ultrasound contrast agent, microvascular flow, elastography and specific imaging processing techniques allows us to obtain improved morphological/functional quantitative information compared to those only derived from B-mode. Precision medicine requires a clear understanding of each patient's heterogeneity and individual situation. Radiological images are often analysed and interpreted by the radiologist only qualitatively (visual evaluation). However digital images are composed of individual pixels to

which discrete brightness or colour values are assigned. They can be efficiently processed, objectively evaluated, and made available at many places at the same time by means of appropriate communication networks and protocols, such as PACS and DICOM protocol. In a digital image, a large amount of numerical data is not analysed by the radiologist. This "hidden" information can be used to create a "radiological plot", which can provide much more information on tissue than simple visual observations by providing objective data. The amount of data associated with digital imaging has increased and produced a large amount of electronic data ("Big Data"). In personalized and precision medicine, the data, analysed with complex mathematical algorithms and the use of artificial intelligence methods (**Figure 6**)¹⁹², can provide quantitative information on pathophysiological phenomena to improve diagnostic accuracy and prognostic and predictive imaging capacity.

Artificial intelligence techniques consist of ML systems. The computer receives data and analyses the existing relationships using analysis systems that reproduce the functioning of the nervous system.

The term "radiomics" was defined by Lambin in 2012¹⁹³ as the high-throughput extraction of image features from diagnostic images. The final product is a quantitative feature, measurable and minable, defined as an "imaging biomarker". Biomarkers are indicators of normal biological processes, pathological changes, or pharmaceutical responses to a therapeutic intervention^{194,195}.

Therefore, radiomics represents diagnostic and predictive support that, together with other clinical and genetic investigations, allows the formulation of personalized therapies and the evaluation of treatment response.

The radiomic data are extracted and processed with bioinformatics tools. They can be combined with other patient data (clinical, biohumoral, genetic) to develop models to improve diagnostic, prognostic and predictive accuracies. Although radiomics is a natural extension of computer-aided diagnosis and detection (CAD) systems, it is significantly different from them. CAD systems are usually used for the detection or diagnosis of disease^{196,197} and are directed towards delivering a

single answer (presence or absence of disease). Radiomics is a process designed to extract a large number of quantitative features from digital images to generate pathophysiological hypotheses and provide information on the phenotype and microenvironment. These features, in conjunction with other information, can be correlated with clinical outcomes and used for clinical support. Radiomics has the potential to help with the diagnosis and visualization of lesion heterogeneity and may prove critical in the assessment of prognosis, prediction of response to treatment, and monitoring of disease status. The “omics” concept readily applies to quantitative tomographic imaging on multiple levels (one multi-layer or three-dimensional images from one patient may easily contain millions of voxels). Complex images with high-dimensional data are generated, corresponding to measurable biological characteristics.

Radiomics depicts the goal of precision medicine, in which stable, reproducible and validated molecular biomarkers are used to predict “the right treatment for the right patient at the right time”^{197,198}.

The radiomic process can be divided into five phases¹⁹⁹: 1) Image acquisition and reconstruction, 2) Segmentation and rendering, 3) Feature extraction and qualification, 4) Construction of a database, and 5) Modelling and validation.

The first step in the radiomics algorithm begins with the choice of an image acquisition protocol. This varies according to the clinical end-point. However, image acquisition parameters, including radiation dose, scanning protocol, reconstruction algorithm, and slice thickness, vary widely in routine clinical practice. Therefore, a comparison of the features extracted from different methods of image acquisition is not possible. The radiomic features are generally sensitive to the acquisition protocols used, only some are stable despite the different image reconstruction settings. Significant efforts are required to identify univocal acquisition and reconstruction protocols and to match them between different scanners.

In most patients with carotid stenotic lesions, the volumes of interest can be identified. Furthermore, the subvolumes within atherosclerotic plaque, representative of plaque heterogeneity, can be

analysed separately. With this approach, images with different acquisition parameters can be combined to yield regions with specific combinations of plaque features (cell density, necrotic core, hemorrhage, atherosclerotic fibrous cap, flow velocity, etc). Once the volumes of interest have been identified, the segmentation strategy must be chosen. This point is critical as the resulting feature values depend on the adopted segmentation methods, which should be stable and reproducible. Usually, manual segmentation by expert readers is considered the gold standard, but it is a time-consuming process with high inter-operator variability. Consequently, the best compromise has been identified in CAD systems that work semi-automatically, with subsequent human manual correction. The use of semi-automated methods has also paved the way for three-dimensional (3D) segmentation¹⁹⁸. Volumetric segmentation allows a comprehensive view of the total lesion and burden, a more complete description of the shape and a greater number of points included in the computation of statistical features, leading to more reliable results that do not suffer from sampling errors. Moreover, computer-aided approaches reduce the manual workload and allow fast and reproducible volumetric segmentations in large cohorts of patients¹⁹⁸. From the identified atherosclerotic plaque, multiple quantitative image features can be extracted, including features that describe the characteristics of the region under analysis, such as the histogram of signal intensity, shape and texture, and descriptors of the position and its relationships with surrounding tissues. Features can be "semantic" or "agnostic". Semantic features are those commonly used by radiologists to describe regions of interest with qualitative descriptors such as size and shape. The agnostic features are mathematically extracted indicators that are generally not part of the traditional lexicon of radiologists and can be divided into first- and second-order statistical features¹⁹⁹. The first-order features describe the intensity histogram by extracting features such as the maximum and average values in addition to the causality and asymmetry of the distribution and have the limitation of not providing information on the spatial relations between voxels. This information can be obtained from the statistical features of the second order, which, using texture analysis methods, describe the relations between the signal in a voxel and the signal in the

neighbouring voxels. Overall, each category produces various quantitative parameters that reflect the specific aspects of a lesion. The power of a predictive classifier model is dependent on having sufficient data. A reasonable rule of thumb is that 10 samples (patients) are needed for each feature in a model based on binary classifiers. Furthermore, the best models are those that can accommodate additional clinical or genomic covariates. Radiomics can be performed with as few as 100 patients, although larger data sets provide more power. Radiomic and non-radiomic features should be combined with the prediction target to create a single dataset. After identification, features can be included or excluded from the model. Radiomic features that are well-correlated with routine clinical features (such as symptoms) or features not correlated with the clinical end point are excluded. A predictive model of clinical outcomes is constructed using the features extracted from the data set. Radiomics produces models for assessing the risk of stroke or for estimating the probability of patient survival. Independent validation datasets are needed to confirm the prognostic value of the same radiomic features. Model performance is measured using receiver operating characteristic (ROC) curve analysis, which measures accuracy throughout the range of possible model values and identifies the best cut-off value. The validation of a model must be accompanied by the verification of its reproducibility by repeating the analyses with the same procedures on different data sets. It is therefore important to have a comprehensive and detailed medical image database ²⁰⁰. Multiple articles have focused on ML approaches for the role of image processing in prediction of cardiovascular event and demonstrated that can improve the accuracy of cardiovascular disease prediction and a better predictive capacity than some traditional risk scores^{201–206, 207–210}.

F. Summary and conclusion

Ultrasonography is the first-line imaging modality for the evaluation of atherosclerotic carotid artery disease, as it is non-invasive, cost-effective, readily available, well-tolerated and safe^{211,212}. Anatomic information is provided with traditional B-mode (greyscale) ultrasound, while hemodynamic information is provided with color Doppler, power Doppler and pulsed-wave Doppler technique^{211,212}.

The image quality provided by ultrasound can be enhanced by the use of a contrast agent²¹². The ultrasonographic contrast agent most often used is microbubbles of an inert gas stabilized by an outer shell consisting of phospholipids or albumin (e.g. sulfur hexafluoride or octafluoropropane)²¹². By use of CEUS, the carotid lumen and adventitia are enhanced, therefore making lumen irregularities more prominent and consequently more easily detectable²¹². CEUS compensates for the inherent limitations of Doppler techniques, such as a lower signal-to-noise ratio, lower sensitivity for slow flow and technical artefacts such as Doppler angle dependence, aliasing and overwriting artefacts²¹². Another use of CEUS is the so-called late-phase enhancement, where the ultrasound examination is performed 6 minutes after administration of the contrast material. Late-phase enhancement suggests an increased inflammatory cell load within the plaque, thus representing a possible marker for early plaque rupture²¹².

Progression of total plaque area and total plaque volume with 3-D ultrasound is a more accurate predictor of transient ischemic attacks, stroke and death than the conventional color Doppler techniques²¹³. Furthermore, 3-D ultrasound may evaluate carotid plaque surface and may identify carotid ulcers, which are associated with a higher incidence of long-term stroke or death^{214,215}.

By using multiple different high spatial resolution contrast weightings, MRI/MRA has the advantage of being able to measure all the hallmarks of carotid plaque vulnerability, namely carotid plaque burden, intraplaque hemorrhage, ulcerations, lipid-rich necrotic core and thin or ruptured fibrous cap²¹⁶. These imaging parameters could be included in a clinical risk prediction model to determine a more personalized stroke risk²¹⁶. Advanced plaques characterized by a large lipid-rich

necrotic core and thinning/rupture of the fibrous cap are associated with an increased risk of ischemic cerebrovascular events by 3-fold (95% CI: 1.51-5.95) and almost 6-fold (95% CI: 2.65-13.30), respectively¹¹². Moreover, intraplaque hemorrhage on MRI is a strong and independent predictor for ipsilateral stroke (Hazard Ratio: 11.0; 95% CI: 4.8 to 25.1)¹²³. MRI provides excellent soft tissue contrast, no ionizing radiation and is not subject to technical challenges such as shadowing or blooming artefacts caused by calcium deposits²¹⁷. MRI is well-validated, highly reproducible and is recognized as the optimal imaging modality for non-invasive assessment of plaque composition for stroke prediction²¹⁷.

CTA is less operator-dependent than carotid ultrasound and is also more quickly performed and more widely available than MRI²¹⁸. CTA evidence of a low-attenuation or “soft” plaque, an increased common carotid artery wall thickness or plaque ulceration strongly correlate with a recent ipsilateral transient ischemic attack or stroke episode²¹⁸. Evaluation of the presence of a soft or calcified plaque, plaque ulceration or increased common carotid artery wall thickness can be easily performed with high reproducibility without requiring lengthy interpretive time or postprocessing software²¹⁸. A recent study demonstrated that CTA may accurately identify specific markers which are more predictive of future stroke risk than the percentage luminal stenosis, such as the presence of intraluminal thrombus, the maximum soft plaque thickness and a thin adventitial calcification (the “rim sign”)²¹⁹. Thin peripheral calcification may be a marker of chronic adventitial inflammation and adventitial microvessel leakage has been implicated in carotid intraplaque hemorrhage²²⁰. These findings highlight the ability of CTA to identify plaque features that are strongly associated with cerebrovascular ischemia.

Identification of IPH using MRI, the presence of carotid ulceration, plaque echolucency on Duplex ultrasound and reduced cerebrovascular reserve are reliable predictors of future cerebrovascular events and may be used to identify high-risk patient subgroups and offer them a prophylactic carotid intervention²²¹. The 2018 European Society for Vascular Surgery (ESVS) guidelines for the management of patients with carotid artery stenosis recommended that in “average surgical risk” patients with a 60-99% ACS, CEA should (Class IIa; Level of Evidence: B) or CAS may be considered (Class IIb; Level of Evidence: B) in the presence of one or more clinical/imaging characteristics that may be associated with an increased risk of late ipsilateral stroke, provided documented perioperative stroke/death rates are <3% and the patient’s life expectancy is >5 years²²². These clinical/imaging characteristics included silent embolic infarcts on brain CTA/MRI, progression in the severity of ACS, a history of contralateral TIA/stroke, microemboli detection on TCD, the presence of IPH on MRI, plaque ulceration on 3D ultrasound or MRI, reduced cerebrovascular reserve, a large plaque area (>40 mm²) on ultrasound longitudinal images and plaque echolucency as shown by a low GSM (<30) and presence of a large (>8 mm²) juxtaluminal hypoechoic area after image normalization of Duplex ultrasound images²²². A recent multinational survey of current practice in carotid imaging reported that the first exam used to evaluate carotid bifurcation disease in ACS patients was ultrasound in 88.8% of respondents, CTA in 7% and MRA in 4.2%²²³. Nevertheless, it is worth mentioning that the percentage luminal stenosis for which CEA or CAS was recommended for asymptomatic patients was reduced in the presence of imaging evidence of “vulnerable plaque features” by a third of study participants (n = 76 of 223 respondents; 34.2%)²²³.

In conclusion, each imaging technique has its own advantages and disadvantages when compared with the other available modalities. Issues like cost-effectiveness, availability, reproducibility of the results and local expertise play an important role, but overall ultrasound should be considered as the

initial imaging modality, followed by CTA or carotid MRA as second line imaging options. The presence or lack of specific imaging parameters should aid physicians and surgeons in their decision-making and the selection of the optimal therapeutic approach for each patient, after also considering each individual patient's views, needs and expectations²²⁴. There is an urgent need for modernized clinical prediction models that include imaging parameters on plaque vulnerability to determine a personalized stroke risk. Trials are warranted to investigate whether including these imaging parameters in clinical decision-making reduces stroke risk and improves the outcome of the patients.

References

1. Bos D, van Dam-Nolen DHK, Gupta A, et al. Advances in Multimodality Carotid Plaque Imaging: AJR Expert Panel Narrative Review. *AJR Am J Roentgenol*. 2021;217(1):16-26. doi:10.2214/AJR.20.24869
2. Chen G, Xue Y, Wei J, Duan Q. The undiagnosed potential clinically significant incidental findings of neck CTA: A large retrospective single-center study. *Medicine (Baltimore)*. 2020;99(43):e22440-e22440. doi:10.1097/MD.00000000000022440
3. AbuRahma AF, Avgerinos ED, Chang RW, et al. Society for Vascular Surgery clinical practice guidelines for management of extracranial cerebrovascular disease. *J Vasc Surg*. 2022;75(1S):4S-22S. doi:10.1016/j.jvs.2021.04.073
4. Barlinn K, Rickmann H, Kitzler H, et al. Validation of Multiparametric Ultrasonography Criteria with Digital Subtraction Angiography in Carotid Artery Disease: A Prospective Multicenter Study. *Ultraschall Med*. 2018;39(5):535-543. doi:10.1055/s-0043-119355
5. Jahromi AS, Cinà CS, Liu Y, Clase CM. Sensitivity and specificity of color duplex ultrasound measurement in the estimation of internal carotid artery stenosis: a systematic review and meta-analysis. *J Vasc Surg*. 2005;41(6):962-972. doi:10.1016/j.jvs.2005.02.044
6. Aboyans V, Ricco J-B, Bartelink M-LEL, et al. 2017 ESC Guidelines on the Diagnosis and Treatment of Peripheral Arterial Diseases, in collaboration with the European Society for Vascular Surgery (ESVS): Document covering atherosclerotic disease of extracranial carotid and vertebral, mesenteric, renal. *Eur Heart J*. 2018;39(9):763-816. doi:10.1093/eurheartj/ehx095
7. Hirt LS. Progression rate and ipsilateral neurological events in asymptomatic carotid stenosis. *Stroke*. 2014;45(3):702-706. doi:10.1161/STROKEAHA.111.613711
8. Kakkos SK, Nicolaidis AN, Charalambous I, et al. Predictors and clinical significance of progression or regression of asymptomatic carotid stenosis. *J Vasc Surg*. 2014;59(4):956-967.e1. doi:10.1016/j.jvs.2013.10.073

9. Mantella LE, Liblik K, Johri AM. Vascular imaging of atherosclerosis: Strengths and weaknesses. *Atherosclerosis*. 2021;319:42-50. doi:10.1016/j.atherosclerosis.2020.12.021
10. Spanos K, Tzorbatzoglou I, Lazari P, Maras D, Giannoukas AD. Carotid artery plaque echomorphology and its association with histopathologic characteristics. *J Vasc Surg*. 2018;68(6):1772-1780. doi:10.1016/j.jvs.2018.01.068
11. Gupta A, Kesavabhotla K, Baradaran H, et al. Plaque echolucency and stroke risk in asymptomatic carotid stenosis: a systematic review and meta-analysis. *Stroke*. 2015;46(1):91-97. doi:10.1161/STROKEAHA.114.006091
12. Nicolaides AN, Kakkos SK, Kyriacou E, et al. Asymptomatic internal carotid artery stenosis and cerebrovascular risk stratification. *J Vasc Surg*. 2010;52(6):1485-1486. doi:10.1016/j.jvs.2010.07.021
13. Salem MK, Bown MJ, Sayers RD, et al. Identification of patients with a histologically unstable carotid plaque using ultrasonic plaque image analysis. *Eur J Vasc Endovasc Surg Off J Eur Soc Vasc Surg*. 2014;48(2):118-125. doi:10.1016/j.ejvs.2014.05.015
14. Brinjikji W, Rabinstein AA, Lanzino G, et al. Ultrasound Characteristics of Symptomatic Carotid Plaques: A Systematic Review and Meta-Analysis. *Cerebrovasc Dis*. 2015;40(3-4):165-174. doi:10.1159/000437339
15. van Engelen A, Wannarong T, Parraga G, et al. Three-dimensional carotid ultrasound plaque texture predicts vascular events. *Stroke*. 2014;45(9):2695-2701. doi:10.1161/STROKEAHA.114.005752
16. Spence JD. Measurement of carotid plaque burden. *Curr Opin Lipidol*. 2020;31(5):291-298. doi:10.1097/MOL.0000000000000706
17. Sillesen H, Sartori S, Sandholt B, Baber U, Mehran R, Fuster V. Carotid plaque thickness and carotid plaque burden predict future cardiovascular events in asymptomatic adult Americans. *Eur Hear journal Cardiovasc Imaging*. 2018;19(9):1042-1050. doi:10.1093/ehjci/jex239

18. Baber U, Mehran R, Sartori S, et al. Prevalence, impact, and predictive value of detecting subclinical coronary and carotid atherosclerosis in asymptomatic adults: the BioImage study. *J Am Coll Cardiol*. 2015;65(11):1065-1074. doi:10.1016/j.jacc.2015.01.017
19. Gudmundsson EF, Björnsdóttir G, Sigurdsson S, et al. Carotid plaque is strongly associated with coronary artery calcium and predicts incident coronary heart disease in a population-based cohort. *Atherosclerosis*. 2022;346:117-123. doi:10.1016/j.atherosclerosis.2022.01.018
20. Näslund U, Ng N, Lundgren A, et al. Visualization of asymptomatic atherosclerotic disease for optimum cardiovascular prevention (VIPVIZA): a pragmatic, open-label, randomised controlled trial. *Lancet (London, England)*. 2019;393(10167):133-142. doi:10.1016/S0140-6736(18)32818-6
21. Spence JD, Coates V, Li H, et al. Effects of intensive medical therapy on microemboli and cardiovascular risk in asymptomatic carotid stenosis. *Arch Neurol*. 2010;67(2):180-186. doi:10.1001/archneurol.2009.289
22. Pérez HA, Adeoye AO, Aballay L, Armando LA, García NH. An intensive follow-up in subjects with cardiometabolic high-risk. *Nutr Metab Cardiovasc Dis*. 2021;31(10):2860-2869. doi:10.1016/j.numecd.2021.06.011
23. Adams A, Bojara W, Romanens M. Effect of Statin Treatment in Patients With Advanced Carotid Atherosclerosis: An Observational Outcome Study. *Cardiol Res*. 2021;12(6):335-339. doi:10.14740/cr1318
24. Spence JD, Hackam DG. Treating arteries instead of risk factors: a paradigm change in management of atherosclerosis. *Stroke*. 2010;41(6):1193-1199. doi:10.1161/STROKEAHA.110.577973
25. Spence JD. Genetics of atherosclerosis: the power of plaque burden and progression: invited commentary on Dong C, Beecham A, Wang L, Blanton SH, Rundek T, Sacco RL. Follow-Up association study of linkage regions reveals multiple candidate genes for carotid plaque i. *Atherosclerosis*. 2012;223(1):98-101. doi:10.1016/j.atherosclerosis.2012.03.040

26. Bogiatzi C, Gloor G, Allen-Vercoe E, et al. Metabolic products of the intestinal microbiome and extremes of atherosclerosis. *Atherosclerosis*. 2018;273:91-97.
doi:10.1016/j.atherosclerosis.2018.04.015
27. Ainsworth CD, Blake CC, Tamayo A, Beletsky V, Fenster A, Spence JD. 3D ultrasound measurement of change in carotid plaque volume: a tool for rapid evaluation of new therapies. *Stroke*. 2005;36(9):1904-1909. doi:10.1161/01.STR.0000178543.19433.20
28. Zhou R, Fenster A, Xia Y, Spence JD, Ding M. Deep learning-based carotid media-adventitia and lumen-intima boundary segmentation from three-dimensional ultrasound images. *Med Phys*. 2019;46(7):3180-3193. doi:10.1002/mp.13581
29. Zhou R, Guo F, Azarpazhooh MR, et al. A Voxel-Based Fully Convolution Network and Continuous Max-Flow for Carotid Vessel-Wall-Volume Segmentation From 3D Ultrasound Images. *IEEE Trans Med Imaging*. 2020;39(9):2844-2855. doi:10.1109/TMI.2020.2975231
30. Zhou R, Guo F, Azarpazhooh MR, et al. Deep Learning-Based Measurement of Total Plaque Area in B-Mode Ultrasound Images. *IEEE J Biomed Heal informatics*. 2021;25(8):2967-2977. doi:10.1109/JBHI.2021.3060163
31. Russell D, Madden KP, Clark WM, Sandset PM, Zivin JA. Detection of arterial emboli using Doppler ultrasound in rabbits. *Stroke*. 1991;22(2):253—258. doi:10.1161/01.str.22.2.253
32. Ringelstein EB, Droste DW, Babikian VL, et al. Consensus on microembolus detection by TCD. International Consensus Group on Microembolus Detection. *Stroke*. 1998;29(3):725-729. doi:10.1161/01.str.29.3.725
33. Kaposzta Z, Young E, Bath PM, Markus HS. Clinical application of asymptomatic embolic signal detection in acute stroke: a prospective study. *Stroke*. 1999;30(9):1814-1818.
doi:10.1161/01.str.30.9.1814
34. Molloy J, Markus HS. Asymptomatic embolization predicts stroke and TIA risk in patients with carotid artery stenosis. *Stroke*. 1999;30(7):1440-1443. doi:10.1161/01.str.30.7.1440
35. Sitzer M, Müller W, Siebler M, et al. Plaque ulceration and lumen thrombus are the main

sources of cerebral microemboli in high-grade internal carotid artery stenosis. *Stroke*. 1995;26(7):1231-1233. doi:10.1161/01.str.26.7.1231

36. Markus HS, King A, Shipley M, et al. Asymptomatic embolisation for prediction of stroke in the Asymptomatic Carotid Emboli Study (ACES): a prospective observational study. *Lancet Neurol*. 2010;9(7):663-671. doi:10.1016/S1474-4422(10)70120-4
37. King A, Markus HS. Doppler embolic signals in cerebrovascular disease and prediction of stroke risk: a systematic review and meta-analysis. *Stroke*. 2009;40(12):3711-3717. doi:10.1161/STROKEAHA.109.563056
38. Markus HS, Droste DW, Kaps M, et al. Dual antiplatelet therapy with clopidogrel and aspirin in symptomatic carotid stenosis evaluated using doppler embolic signal detection: the Clopidogrel and Aspirin for Reduction of Emboli in Symptomatic Carotid Stenosis (CARESS) trial. *Circulation*. 2005;111(17):2233-2240. doi:10.1161/01.CIR.0000163561.90680.1C
39. Best LMJ, Webb AC, Gurusamy KS, Cheng SF, Richards T. Transcranial Doppler Ultrasound Detection of Microemboli as a Predictor of Cerebral Events in Patients with Symptomatic and Asymptomatic Carotid Disease: A Systematic Review and Meta-Analysis. *Eur J Vasc Endovasc Surg Off J Eur Soc Vasc Surg*. 2016;52(5):565-580. doi:10.1016/j.ejvs.2016.05.019
40. Topakian R, King A, Kwon SU, Schaafsma A, Shipley M, Markus HS. Ultrasonic plaque echolucency and emboli signals predict stroke in asymptomatic carotid stenosis. *Neurology*. 2011;77(8):751-758. doi:10.1212/WNL.0b013e31822b00a6
41. Goertler M, Baeumer M, Kross R, et al. Rapid decline of cerebral microemboli of arterial origin after intravenous acetylsalicylic acid. *Stroke*. 1999;30(1):66-69. doi:10.1161/01.str.30.1.66
42. Johnston SC, Easton JD, Farrant M, et al. Clopidogrel and Aspirin in Acute Ischemic Stroke and High-Risk TIA. *N Engl J Med*. 2018;379(3):215-225. doi:10.1056/NEJMoa1800410

43. Safouris A, Krogias C, Sharma VK, et al. Statin Pretreatment and Microembolic Signals in Large Artery Atherosclerosis. *Arterioscler Thromb Vasc Biol.* 2017;37(7):1415-1422. doi:10.1161/ATVBAHA.117.309292
44. Wang Y, Wang Y, Zhao X, et al. Clopidogrel with aspirin in acute minor stroke or transient ischemic attack. *N Engl J Med.* 2013;369(1):11-19. doi:10.1056/NEJMoa1215340
45. Staub D, Partovi S, Imfeld S, et al. Novel applications of contrast-enhanced ultrasound imaging in vascular medicine. *Vasa.* 2013;42(1):17-31. doi:10.1024/0301-1526/a000244
46. Staub D, Schinkel AFL, Coll B, et al. Contrast-enhanced ultrasound imaging of the vasa vasorum: from early atherosclerosis to the identification of unstable plaques. *JACC Cardiovasc Imaging.* 2010;3(7):761-771. doi:10.1016/j.jcmg.2010.02.007
47. Rafailidis V, Li X, Sidhu PS, Partovi S, Staub D. Contrast imaging ultrasound for the detection and characterization of carotid vulnerable plaque. *Cardiovasc Diagn Ther.* 2020;10(4):965-981. doi:10.21037/cdt.2020.01.08
48. Schinkel AFL, Bosch JG, Staub D, Adam D, Feinstein SB. Contrast-Enhanced Ultrasound to Assess Carotid Intraplaque Neovascularization. *Ultrasound Med Biol.* 2020;46(3):466-478. doi:10.1016/j.ultrasmedbio.2019.10.020
49. Rafailidis V, Chrysogonidis I, Xerras C, et al. A comparative study of color Doppler imaging and contrast-enhanced ultrasound for the detection of ulceration in patients with carotid atherosclerotic disease. *Eur Radiol.* 2019;29(4):2137-2145. doi:10.1007/s00330-018-5773-8
50. Rafailidis V, Chrysogonidis I, Xerras C, et al. An Ultrasonographic Multiparametric Carotid Plaque Risk Index Associated with Cerebrovascular Symptomatology: A Study Comparing Color Doppler Imaging and Contrast-Enhanced Ultrasonography. *AJNR Am J Neuroradiol.* 2019;40(6):1022-1028. doi:10.3174/ajnr.A6056
51. Staub D, Partovi S, Schinkel AFL, et al. Correlation of carotid artery atherosclerotic lesion echogenicity and severity at standard US with intraplaque neovascularization detected at

- contrast-enhanced US. *Radiology*. 2011;258(2):618-626. doi:10.1148/radiol.10101008
52. Staub D, Patel MB, Tibrewala A, et al. Vasa vasorum and plaque neovascularization on contrast-enhanced carotid ultrasound imaging correlates with cardiovascular disease and past cardiovascular events. *Stroke*. 2010;41(1):41-47.
doi:10.1161/STROKEAHA.109.560342
53. Li C, He W, Guo D, et al. Quantification of carotid plaque neovascularization using contrast-enhanced ultrasound with histopathologic validation. *Ultrasound Med Biol*. 2014;40(8):1827-1833. doi:10.1016/j.ultrasmedbio.2014.02.010
54. van den Oord SCH, Akkus Z, Bosch JG, et al. Quantitative contrast-enhanced ultrasound of intraplaque neovascularization in patients with carotid atherosclerosis. *Ultraschall Med*. 2015;36(2):154-161. doi:10.1055/s-0034-1366410
55. Kaspar M, Baumgartner I, Staub D, Drexel H, Thalhammer C. Non-invasive ultrasound-based imaging of atherosclerosis. *Vasa*. 2019;48(2):126-133. doi:10.1024/0301-1526/a000747
56. Coli S, Magnoni M, Sangiorgi G, et al. Contrast-enhanced ultrasound imaging of intraplaque neovascularization in carotid arteries: correlation with histology and plaque echogenicity. *J Am Coll Cardiol*. 2008;52(3):223-230. doi:10.1016/j.jacc.2008.02.082
57. Hoogi A, Adam D, Hoffman A, Kerner H, Reisner S, Gaitini D. Carotid plaque vulnerability: quantification of neovascularization on contrast-enhanced ultrasound with histopathologic correlation. *AJR Am J Roentgenol*. 2011;196(2):431-436. doi:10.2214/AJR.10.4522
58. Schmidt C, Fischer T, Rückert R-I, et al. Identification of neovascularization by contrast-enhanced ultrasound to detect unstable carotid stenosis. *PLoS One*. 2017;12(4):e0175331. doi:10.1371/journal.pone.0175331
59. Yan H, Wu X, He Y, Staub D, Wen X, Luo Y. Carotid Intraplaque Neovascularization on Contrast-Enhanced Ultrasound Correlates with Cardiovascular Events and Poor Prognosis: A Systematic Review and Meta-analysis. *Ultrasound Med Biol*. 2021;47(2):167-176.

doi:10.1016/j.ultrasmedbio.2020.10.013

60. Li Z, Xu X, Ren L, et al. Prospective Study About the Relationship Between CEUS of Carotid Intraplaque Neovascularization and Ischemic Stroke in TIA Patients. *Front Pharmacol.* 2019;10:672. doi:10.3389/fphar.2019.00672
61. Cui L, Xing Y, Zhou Y, et al. Carotid intraplaque neovascularisation as a predictive factor for future vascular events in patients with mild and moderate carotid stenosis: an observational prospective study. *Ther Adv Neurol Disord.* 2021;14:17562864211023992. doi:10.1177/17562864211023992
62. Mantella LE, Colledanchise KN, Héту M-F, Feinstein SB, Abunassar J, Johri AM. Carotid intraplaque neovascularization predicts coronary artery disease and cardiovascular events. *Eur Hear journal Cardiovasc Imaging.* 2019;20(11):1239-1247. doi:10.1093/ehjci/jez070
63. Magnoni M, Ammirati E, Moroni F, Norata GD, Camici PG. Impact of Cardiovascular Risk Factors and Pharmacologic Treatments on Carotid Intraplaque Neovascularization Detected by Contrast-Enhanced Ultrasound. *J Am Soc Echocardiogr Off Publ Am Soc Echocardiogr.* 2019;32(1):113-120.e6. doi:10.1016/j.echo.2018.09.001
64. Anderson GB, Ashforth R, Steinke DE, Ferdinandy R, Findlay JM. CT angiography for the detection and characterization of carotid artery bifurcation disease. *Stroke.* 2000;31(9):2168-2174. doi:10.1161/01.str.31.9.2168
65. Leclerc X, Godefroy O, Pruvo JP, Leys D. Computed tomographic angiography for the evaluation of carotid artery stenosis. *Stroke.* 1995;26(9):1577-1581. doi:10.1161/01.str.26.9.1577
66. Randoux B, Marro B, Koskas F, et al. Carotid artery stenosis: prospective comparison of CT, three-dimensional gadolinium-enhanced MR, and conventional angiography. *Radiology.* 2001;220(1):179-185. doi:10.1148/radiology.220.1.r01j135179
67. Chen C-J, Lee T-H, Hsu H-L, et al. Multi-Slice CT angiography in diagnosing total versus near occlusions of the internal carotid artery: comparison with catheter angiography. *Stroke.*

- 2004;35(1):83-85. doi:10.1161/01.STR.0000106139.38566.B2
68. Koelemay MJW, Nederkoorn PJ, Reitsma JB, Majoie CB. Systematic review of computed tomographic angiography for assessment of carotid artery disease. *Stroke*. 2004;35(10):2306-2312. doi:10.1161/01.STR.0000141426.63959.cc
69. Porsche C, Walker L, Mendelow D, Birchall D. Evaluation of cross-sectional luminal morphology in carotid atherosclerotic disease by use of spiral CT angiography. *Stroke*. 2001;32(11):2511-2515. doi:10.1161/hs1101.098153
70. Dix JE, Evans AJ, Kallmes DF, Sobel AH, Phillips CD. Accuracy and precision of CT angiography in a model of carotid artery bifurcation stenosis. *AJNR Am J Neuroradiol*. 1997;18(3):409-415.
71. Napoli A, Fleischmann D, Chan FP, et al. Computed tomography angiography: state-of-the-art imaging using multidetector-row technology. *J Comput Assist Tomogr*. 2004;28 Suppl 1:S32-45. doi:10.1097/01.rct.0000120859.80935.10
72. Prokop M, Waaijer A, Kreuzer S. CT angiography of the carotid arteries. *JBR-BTR organe la Soc R belge Radiol = orgaan van K Belgische Ver voor Radiol*. 2004;87(1):23-29.
73. Bartlett ES, Walters TD, Symons SP, Fox AJ. Quantification of carotid stenosis on CT angiography. *AJNR Am J Neuroradiol*. 2006;27(1):13-19.
74. Saba L, Saam T, Jäger HR, et al. Imaging biomarkers of vulnerable carotid plaques for stroke risk prediction and their potential clinical implications. *Lancet Neurol*. 2019;4422(19):1-14. doi:10.1016/S1474-4422(19)30035-3
75. Saba L, Anzidei M, Marincola BC, et al. Imaging of the carotid artery vulnerable plaque. *Cardiovasc Intervent Radiol*. 2014;37(3):572-585. doi:10.1007/s00270-013-0711-2
76. Cademartiri F, Balestrieri A, Cau R, et al. Insight from imaging on plaque vulnerability: similarities and differences between coronary and carotid arteries—implications for systemic therapies. *Cardiovasc Diagn Ther*. 2020;10(4):1150-1162. doi:10.21037/cdt-20-528
77. Cau R, Flanders A, Mannelli L, et al. Artificial Intelligence in Computed Tomography

Plaque Characterization: A Review. *Eur J Radiol*. Published online 2021:109767.

doi:<https://doi.org/10.1016/j.ejrad.2021.109767>

78. Michel J-B, Virmani R, Arbustini E, Pasterkamp G. Intraplaque haemorrhages as the trigger of plaque vulnerability. *Eur Heart J*. 2011;32(16):1977-1985, 1985a, 1985b, 1985c.
doi:10.1093/eurheartj/ehr054
79. Saam T, Hetterich H, Hoffmann V, et al. Meta-analysis and systematic review of the predictive value of carotid plaque hemorrhage on cerebrovascular events by magnetic resonance imaging. *J Am Coll Cardiol*. 2013;62(12):1081-1091.
doi:10.1016/j.jacc.2013.06.015
80. Singh N, Moody AR, Panzov V, Gladstone DJ. Carotid Intraplaque Hemorrhage in Patients with Embolic Stroke of Undetermined Source. *J stroke Cerebrovasc Dis Off J Natl Stroke Assoc*. 2018;27(7):1956-1959. doi:10.1016/j.jstrokecerebrovasdis.2018.02.042
81. Saba L, Francone M, Bassareo PP, et al. CT Attenuation Analysis of Carotid Intraplaque Hemorrhage. *AJNR Am J Neuroradiol*. 2018;39(1):131-137. doi:10.3174/ajnr.A5461
82. Eisenmenger LB, Aldred BW, Kim S-E, et al. Prediction of Carotid Intraplaque Hemorrhage Using Adventitial Calcification and Plaque Thickness on CTA. *AJNR Am J Neuroradiol*. 2016;37(8):1496-1503. doi:10.3174/ajnr.A4765
83. Cai J, Hatsukami TS, Ferguson MS, et al. In vivo quantitative measurement of intact fibrous cap and lipid-rich necrotic core size in atherosclerotic carotid plaque: comparison of high-resolution, contrast-enhanced magnetic resonance imaging and histology. *Circulation*. 2005;112(22):3437-3444. doi:10.1161/CIRCULATIONAHA.104.528174
84. Cury RC, Houser SL, Furie KL, et al. Vulnerable plaque detection by 3.0 tesla magnetic resonance imaging. *Invest Radiol*. 2006;41(2):112-115.
doi:10.1097/01.rli.0000186419.55504.30
85. Xu D, Hippe DS, Underhill HR, et al. Prediction of high-risk plaque development and plaque progression with the carotid atherosclerosis score. *JACC Cardiovasc Imaging*.

2014;7(4):366-373. doi:10.1016/j.jcmg.2013.09.022

86. Saba L, Yuan C, Hatsukami TS, et al. Carotid Artery Wall Imaging: Perspective and Guidelines from the ASNR Vessel Wall Imaging Study Group and Expert Consensus Recommendations of the American Society of Neuroradiology. *Am J Neuroradiol*. 2018;39(2). doi:10.3174/ajnr.A5488
87. Saba L, Agarwal N, Cau R, et al. Review of imaging biomarkers for the vulnerable carotid plaque. *JVS Vasc Sci*. Published online 2021. doi:https://doi.org/10.1016/j.jvssci.2021.03.001
88. Cerrone G, Fanni D, Lai ML, et al. Plasma cells in the carotid plaque: Occurrence and significance. *Eur Rev Med Pharmacol Sci*. 2021;25(11):4064-4068.
doi:10.26355/eurrev_202106_26047
89. McCarthy MJ, Loftus IM, Thompson MM, et al. Angiogenesis and the atherosclerotic carotid plaque: an association between symptomatology and plaque morphology. *J Vasc Surg*. 1999;30(2):261-268. doi:10.1016/s0741-5214(99)70136-9
90. Saba L, Lai ML, Montisci R, et al. Association between carotid plaque enhancement shown by multidetector CT angiography and histologically validated microvessel density. *Eur Radiol*. 2012;22(10):2237-2245. doi:10.1007/s00330-012-2467-5
91. Barnett HJ, Taylor DW, Eliasziw M, et al. Benefit of carotid endarterectomy in patients with symptomatic moderate or severe stenosis. North American Symptomatic Carotid Endarterectomy Trial Collaborators. *N Engl J Med*. 1998;339(20):1415-1425.
doi:10.1056/NEJM199811123392002
92. Saba L, Caddeo G, Sanfilippo R, Montisci R, Mallarini G. CT and ultrasound in the study of ulcerated carotid plaque compared with surgical results: potentialities and advantages of multidetector row CT angiography. *AJNR Am J Neuroradiol*. 2007;28(6):1061-1066.
doi:10.3174/ajnr.A0486
93. Saba L, Caddeo G, Sanfilippo R, Montisci R, Mallarini G. Efficacy and sensitivity of axial scans and different reconstruction methods in the study of the ulcerated carotid plaque using

multidetector-row CT angiography: comparison with surgical results. *AJNR Am J Neuroradiol.* 2007;28(4):716-723.

94. Rozie S, de Weert TT, de Monyé C, et al. Atherosclerotic plaque volume and composition in symptomatic carotid arteries assessed with multidetector CT angiography; relationship with severity of stenosis and cardiovascular risk factors. *Eur Radiol.* 2009;19(9):2294-2301. doi:10.1007/s00330-009-1394-6
95. Pini R, Faggioli G, Fittipaldi S, et al. Relationship between Calcification and Vulnerability of the Carotid Plaques. *Ann Vasc Surg.* 2017;44(May):336-342. doi:10.1016/j.avsg.2017.04.017
96. Yang J, Pan X, Zhang B, et al. Superficial and multiple calcifications and ulceration associate with intraplaque hemorrhage in the carotid atherosclerotic plaque. *Eur Radiol.* 2018;28(12):4968-4977. doi:10.1007/s00330-018-5535-7
97. Eisenmenger LB, Aldred BW, Kim SE, et al. Prediction of carotid intraplaque hemorrhage using adventitial calcification and plaque thickness on CTA. *Am J Neuroradiol.* 2016;37(8):1496-1503. doi:10.3174/ajnr.A4765
98. Saba L, Chen H, Cau R, et al. Impact Analysis of Different CT Configurations of Carotid Artery Plaque Calcifications on Cerebrovascular Events. *AJNR Am J Neuroradiol.* 2022;43(2):272-279. doi:10.3174/ajnr.A7401
99. Saba L, Nardi V, Cau R, et al. Carotid Artery Plaque Calcifications: Lessons from Histopathology to Diagnostic Imaging. *Stroke.* 2022;53(1):290-297. doi:10.1161/STROKEAHA.121.035692
100. Baumgartner RW, Arnold M, Baumgartner I, et al. Carotid dissection with and without ischemic events: local symptoms and cerebral artery findings. *Neurology.* 2001;57(5):827-832.
101. Hakimi R, Sivakumar S. Imaging of carotid dissection. *Curr Pain Headache Rep.* 2019;23(1):1-7.
102. Kadian-Dodov D, Gornik HL, Gu X, et al. Dissection and Aneurysm in Patients

- With Fibromuscular Dysplasia: Findings From the U.S. Registry for FMD. *J Am Coll Cardiol*. 2016;68(2):176-185. doi:<https://doi.org/10.1016/j.jacc.2016.04.044>
103. Madaelil TP, Grossberg JA, Nogueira RG, et al. Multimodality Imaging in Carotid Web . *Front Neurol* . 2019;10. <https://www.frontiersin.org/article/10.3389/fneur.2019.00220>
104. Wojcik K, Milburn J, Vidal G, Steven A. Carotid Webs: Radiographic Appearance and Significance. *Ochsner J*. 2018;18(2):115-120. doi:10.31486/toj.18.0001
105. Priyadarshni S, Neralla A, Reimon J, Smithson S. Carotid Webs: An Unusual Presentation of Fibromuscular Dysplasia. *Cureus*. 2020;12(8):e9549-e9549. doi:10.7759/cureus.9549
106. Abdel Razek AAK, Alvarez H, Bagg S, Refaat S, Castillo M. Imaging Spectrum of CNS Vasculitis. *RadioGraphics*. 2014;34(4):873-894. doi:10.1148/rg.344135028
107. Jennette JC, Falk RJ, Bacon PA, et al. 2012 revised International Chapel Hill Consensus Conference Nomenclature of Vasculitides. *Arthritis Rheum*. 2013;65(1):1-11. doi:10.1002/art.37715
108. MRC European Carotid Surgery Trial: interim results for symptomatic patients with severe (70-99%) or with mild (0-29%) carotid stenosis. European Carotid Surgery Trialists' Collaborative Group. *Lancet (London, England)*. 1991;337(8752):1235-1243.
109. Walker MD, Marler JR, Goldstein M, et al. Endarterectomy for Asymptomatic Carotid Artery Stenosis. *JAMA*. 1995;273(18):1421-1428. doi:10.1001/jama.1995.03520420037035
110. Halliday A, Harrison M, Hayter E, et al. 10-year stroke prevention after successful carotid endarterectomy for asymptomatic stenosis (ACST-1): a multicentre randomised trial. *Lancet (London, England)*. 2010;376(9746):1074-1084. doi:10.1016/S0140-6736(10)61197-X
111. Messas E, Goudot G, Halliday A, et al. Management of carotid stenosis for primary and secondary prevention of stroke: state-of-the-art 2020: a critical review. *Eur Heart J Suppl*. 2020;22(Suppl M):M35-M42. doi:10.1093/eurheartj/suaa162
112. Gupta A, Baradaran H, Schweitzer AD, et al. Carotid plaque MRI and stroke risk: a systematic review and meta-analysis. *Stroke*. 2013;44(11):3071-3077.

doi:10.1161/STROKEAHA.113.002551

113. Wasserman BA. Advanced Contrast-Enhanced MRI for Looking Beyond the Lumen to Predict Stroke. *Stroke*. 2010;41(10_suppl_1):S12-S16.
doi:10.1161/STROKEAHA.110.596288
114. Wasserman BA, Wityk RJ, Trout HH, Virmani R. Low-grade carotid stenosis: Looking beyond the lumen with MRI. *Stroke*. 2005;36(11):2504-2513.
doi:10.1161/01.STR.0000185726.83152.00
115. O'Leary DH, Polak JF, Kronmal RA, et al. Distribution and correlates of sonographically detected carotid artery disease in the Cardiovascular Health Study. The CHS Collaborative Research Group. *Stroke*. 1992;23(12):1752-1760. doi:10.1161/01.str.23.12.1752
116. Astor BC, Sharrett AR, Coresh J, Chambless LE, Wasserman BA. Remodeling of carotid arteries detected with MR imaging: atherosclerosis risk in communities carotid MRI study. *Radiology*. 2010;256(3):879-886. doi:10.1148/radiol.10091162
117. Babiarz LS, Astor B, Mohamed MA, Wasserman BA. Comparison of Gadolinium-Enhanced Cardiovascular Magnetic Resonance Angiography with High-Resolution Black Blood Cardiovascular Magnetic Resonance for Assessing Carotid Artery Stenosis. *J Cardiovasc Magn Reson*. 2007;9(1):63-70. doi:10.1080/10976640600843462
118. Cai JM, Hatsukami TS, Ferguson MS, Small R, Polissar NL, Yuan C. Classification of human carotid atherosclerotic lesions with in vivo multicontrast magnetic resonance imaging. *Circulation*. 2002;106(11):1368-1373. doi:10.1161/01.CIR.0000028591.44554.F9
119. Saba L, Moody AR, Saam T, et al. Vessel Wall-Imaging Biomarkers of Carotid Plaque Vulnerability in Stroke Prevention Trials: A viewpoint from The Carotid Imaging Consensus Group. *JACC Cardiovasc Imaging*. 2020;13(11):2445-2456.
doi:10.1016/j.jcmg.2020.07.046
120. Saba L, Saam T, Jäger HR, et al. Imaging biomarkers of vulnerable carotid plaques for stroke risk prediction and their potential clinical implications. *Lancet Neurol*. 2019;18(6):559-572.

doi:10.1016/S1474-4422(19)30035-3

121. Saba L, Brinjikji W, Spence JD, et al. Roadmap Consensus on Carotid Artery Plaque Imaging and Impact on Therapy Strategies and Guidelines: An International, Multispecialty, Expert Review and Position Statement. *AJNR Am J Neuroradiol*. 2021;42(9):1566-1575.
doi:10.3174/ajnr.A7223
122. Cappendijk VC, Cleutjens KBJM, Heeneman S, et al. In vivo detection of hemorrhage in human atherosclerotic plaques with magnetic resonance imaging. *J Magn Reson Imaging*. 2004;20(1):105-110. doi:10.1002/jmri.20060
123. Schindler A, Schinner R, Altaf N, et al. Prediction of Stroke Risk by Detection of Hemorrhage in Carotid Plaques: Meta-Analysis of Individual Patient Data. *JACC Cardiovasc Imaging*. 2020;13(2 Pt 1):395-406. doi:10.1016/j.jcmg.2019.03.028
124. Kamel H, Merkler AE, Iadecola C, Gupta A, Navi BB. Tailoring the Approach to Embolic Stroke of Undetermined Source: A Review. *JAMA Neurol*. 2019;76(7):855-861.
doi:10.1001/jamaneurol.2019.0591
125. Kamel H, Navi BB, Merkler AE, et al. Reclassification of Ischemic Stroke Etiological Subtypes on the Basis of High-Risk Nonstenosing Carotid Plaque. *Stroke*. 2020;51(2):504-510. doi:10.1161/STROKEAHA.119.027970
126. Baradaran H, Patel P, Gialdini G, et al. Quantifying Intracranial Internal Carotid Artery Stenosis on MR Angiography. *AJNR Am J Neuroradiol*. 2017;38(5):986-990.
doi:10.3174/ajnr.A5113
127. Hirai T, Korogi Y, Ono K, et al. Prospective evaluation of suspected stenocclusive disease of the intracranial artery: combined MR angiography and CT angiography compared with digital subtraction angiography. *AJNR Am J Neuroradiol*. 2002;23(1):93-101.
128. Degnan AJ, Gallagher G, Teng Z, Lu J, Liu Q, Gillard JH. MR angiography and imaging for the evaluation of middle cerebral artery atherosclerotic disease. *AJNR Am J Neuroradiol*. 2012;33(8):1427-1435. doi:10.3174/ajnr.A2697

129. Lehman VT, Brinjikji W, Kallmes DF, et al. Clinical interpretation of high-resolution vessel wall MRI of intracranial arterial diseases. *Br J Radiol*. 2016;89(1067):20160496. doi:10.1259/bjr.20160496
130. Lindenholz A, van der Kolk AG, Zwanenburg JJM, Hendrikse J. The Use and Pitfalls of Intracranial Vessel Wall Imaging: How We Do It. *Radiology*. 2018;286(1):12-28. doi:10.1148/radiol.2017162096
131. Mandell DM, Mossa-Basha M, Qiao Y, et al. Intracranial Vessel Wall MRI: Principles and Expert Consensus Recommendations of the American Society of Neuroradiology. *AJNR Am J Neuroradiol*. 2017;38(2):218-229. doi:10.3174/ajnr.A4893
132. Wang Y, Liu X, Wu X, Degnan AJ, Malhotra A, Zhu C. Culprit intracranial plaque without substantial stenosis in acute ischemic stroke on vessel wall MRI: A systematic review. *Atherosclerosis*. 2019;287:112-121. doi:10.1016/j.atherosclerosis.2019.06.907
133. Zhao M, Amin-Hanjani S, Ruland S, Curcio AP, Ostergren L, Charbel FT. Regional cerebral blood flow using quantitative MR angiography. *AJNR Am J Neuroradiol*. 2007;28(8):1470-1473. doi:10.3174/ajnr.A0582
134. Wehrum T, Dragonu I, Strecker C, et al. Aortic atheroma as a source of stroke - assessment of embolization risk using 3D CMR in stroke patients and controls. *J Cardiovasc Magn Reson Off J Soc Cardiovasc Magn Reson*. 2017;19(1):67. doi:10.1186/s12968-017-0379-x
135. Cocker MS, Spence JD, Hammond R, et al. [(18)F]-NaF PET/CT Identifies Active Calcification in Carotid Plaque. *JACC Cardiovasc Imaging*. 2017;10(4):486-488. doi:10.1016/j.jcmg.2016.03.005
136. Evans NR, Tarkin JM, Le EP, et al. Integrated cardiovascular assessment of atherosclerosis using PET/MRI. *Br J Radiol*. 2020;93(1113):20190921. doi:10.1259/bjr.20190921
137. Aizaz M, Moonen RPM, van der Pol JAJ, Prieto C, Botnar RM, Kooi ME. PET/MRI of atherosclerosis. *Cardiovasc Diagn Ther*. 2020;10(4):1120-1139. doi:10.21037/cdt.2020.02.09

138. Rudd JHF, Warburton EA, Fryer TD, et al. Imaging atherosclerotic plaque inflammation with [18F]-fluorodeoxyglucose positron emission tomography. *Circulation*. 2002;105(23):2708-2711. doi:10.1161/01.cir.0000020548.60110.76
139. Bucnerius J, Hyafil F, Verberne HJ, et al. Position paper of the Cardiovascular Committee of the European Association of Nuclear Medicine (EANM) on PET imaging of atherosclerosis. *Eur J Nucl Med Mol Imaging*. 2016;43(4):780-792. doi:10.1007/s00259-015-3259-3
140. Cocker MS, Spence JD, Hammond R, et al. [18F]-Fluorodeoxyglucose PET/CT imaging as a marker of carotid plaque inflammation: Comparison to immunohistology and relationship to acuity of events. *Int J Cardiol*. 2018;271:378-386. doi:10.1016/j.ijcard.2018.05.057
141. Kwee RM, Truijman MTB, Mess WH, et al. Potential of Integrated [¹⁸F] Fluorodeoxyglucose Positron-Emission Tomography/CT in Identifying Vulnerable Carotid Plaques. *Am J Neuroradiol*. 2011;32(5):950 LP - 954. doi:10.3174/ajnr.A2381
142. Chaker S, Al-Dasuqi K, Baradaran H, et al. Carotid Plaque Positron Emission Tomography Imaging and Cerebral Ischemic Disease. *Stroke*. 2019;50(8):2072-2079. doi:10.1161/STROKEAHA.118.023987
143. Poredos P, Spirkoska A, Lezaic L, Mijovski MB, Jezovnik MK. Patients with an Inflamed Atherosclerotic Plaque have Increased Levels of Circulating Inflammatory Markers. *J Atheroscler Thromb*. 2017;24(1):39-46. doi:10.5551/jat.34884
144. Jezovnik MK, Zidar N, Lezaic L, Gersak B, Poredos P. Identification of inflamed atherosclerotic lesions in vivo using PET-CT. *Inflammation*. 2014;37(2):426-434. doi:10.1007/s10753-013-9755-3
145. Truijman MTB, Kwee RM, van Hoof RHM, et al. Combined 18F-FDG PET-CT and DCE-MRI to assess inflammation and microvascularization in atherosclerotic plaques. *Stroke*. 2013;44(12):3568-3570. doi:10.1161/STROKEAHA.113.003140
146. Wang J, Liu H, Sun J, et al. Varying correlation between 18F-fluorodeoxyglucose positron

emission tomography and dynamic contrast-enhanced MRI in carotid atherosclerosis: implications for plaque inflammation. *Stroke*. 2014;45(6):1842-1845.

doi:10.1161/STROKEAHA.114.005147

147. Tarkin JM, Joshi FR, Evans NR, et al. Detection of Atherosclerotic Inflammation by (68)Ga-DOTATATE PET Compared to [(18)F]FDG PET Imaging. *J Am Coll Cardiol*. 2017;69(14):1774-1791. doi:10.1016/j.jacc.2017.01.060
148. Gaemperli O, Shalhoub J, Owen DRJ, et al. Imaging intraplaque inflammation in carotid atherosclerosis with 11C-PK11195 positron emission tomography/computed tomography. *Eur Heart J*. 2012;33(15):1902-1910. doi:10.1093/eurheartj/ehr367
149. Vöö S, Kwee RM, Sluimer JC, et al. Imaging Intraplaque Inflammation in Carotid Atherosclerosis With 18F-Fluorocholine Positron Emission Tomography-Computed Tomography: Prospective Study on Vulnerable Atheroma With Immunohistochemical Validation. *Circ Cardiovasc Imaging*. 2016;9(5). doi:10.1161/CIRCIMAGING.115.004467
150. Vesey AT, Jenkins WSA, Irkle A, et al. (18)F-Fluoride and (18)F-Fluorodeoxyglucose Positron Emission Tomography After Transient Ischemic Attack or Minor Ischemic Stroke: Case-Control Study. *Circ Cardiovasc Imaging*. 2017;10(3):e004976. doi:10.1161/CIRCIMAGING.116.004976
151. Joshi N V, Vesey AT, Williams MC, et al. 18F-fluoride positron emission tomography for identification of ruptured and high-risk coronary atherosclerotic plaques: a prospective clinical trial. *Lancet (London, England)*. 2014;383(9918):705-713. doi:10.1016/S0140-6736(13)61754-7
152. Mizuno K TM. *Coronary Angioscopy*. Springer Japan; <https://books.google.com/books?id=b7MYCgAAQBAJ>
153. Uchida Y. Recent advances in coronary angioscopy. *J Cardiol*. 2011;57(1):18-30. doi:10.1016/j.jjcc.2010.11.001
154. Savastano LE, Seibel EJ. Scanning Fiber Angioscopy: A Multimodal Intravascular Imaging

Platform for Carotid Atherosclerosis. *Neurosurgery*. 2017;64(CN_suppl_1):188-198.

doi:10.1093/neuros/nyx322

155. Savastano LE, Zhou Q, Smith A, et al. Multimodal laser-based angioscopy for structural, chemical and biological imaging of atherosclerosis. *Nat Biomed Eng*. 2017;1(2):23.
doi:10.1038/s41551-016-0023
156. Kan P, Mokin M, Abila AA, et al. Utility of intravascular ultrasound in intracranial and extracranial neurointerventions: experience at University at Buffalo Neurosurgery-Millard Fillmore Gates Circle Hospital. *Neurosurg Focus*. 2012;32(1):E6.
doi:10.3171/2011.10.FOCUS11242
157. Sangiorgi G, Bedogni F, Sganzerla P, et al. The Virtual histology In Carotids Observational Registry (VICTORY) study: A European prospective registry to assess the feasibility and safety of intravascular ultrasound and virtual histology during carotid interventions. *Int J Cardiol*. 2013;168(3):2089-2093. doi:10.1016/j.ijcard.2013.01.159
158. Diethrich EB, Paulina Margolis M, Reid DB, et al. Virtual histology intravascular ultrasound assessment of carotid artery disease: the Carotid Artery Plaque Virtual Histology Evaluation (CAPITAL) study. *J Endovasc Ther an Off J Int Soc Endovasc Spec*. 2007;14(5):676-686. doi:10.1177/152660280701400512
159. Funatsu N, Enomoto Y, Egashira Y, et al. Tissue Protrusion With Attenuation Is Associated With Ischemic Brain Lesions After Carotid Artery Stenting. *Stroke*. 2020;51(1):327-330.
doi:10.1161/STROKEAHA.119.026332
160. de Donato G, Pasqui E, Alba G, et al. Clinical considerations and recommendations for OCT-guided carotid artery stenting. *Expert Rev Cardiovasc Ther*. 2020;18(4):219-229.
doi:10.1080/14779072.2020.1756777
161. Roth GA, Johnson C, Abajobir A, et al. Global, Regional, and National Burden of Cardiovascular Diseases for 10 Causes, 1990 to 2015. *J Am Coll Cardiol*. 2017;70(1):1-25.
doi:10.1016/j.jacc.2017.04.052

162. Feigin VL, Norrving B, Mensah GA. Global Burden of Stroke. *Circ Res*. 2017;120(3):439-448. doi:10.1161/CIRCRESAHA.116.308413
163. Cau R, Cherchi V, Micheletti G, et al. Potential Role of Artificial Intelligence in Cardiac Magnetic Resonance Imaging. *J Thorac Imaging*. 2021;Publish Ah(3):142-148. doi:10.1097/rti.0000000000000584
164. Cau R, Faa G, Nardi V, et al. Long-COVID diagnosis: From diagnostic to advanced AI-driven models. *Eur J Radiol*. 2022;148(January):110164. doi:10.1016/j.ejrad.2022.110164
165. Shishikura D. Noninvasive imaging modalities to visualize atherosclerotic plaques. *Cardiovasc Diagn Ther*. 2016;6(4):340-353. doi:10.21037/cdt.2015.11.07
166. Paraskevas KI, Nicolaides AN, Kakkos SK. Asymptomatic Carotid Stenosis and Risk of Stroke (ACSRS) study: what have we learned from it? *Ann Transl Med*. 2020;8(19):1271. doi:10.21037/atm.2020.02.156
167. Kakkos SK, Griffin MB, Nicolaides AN, et al. The size of juxtaluminal hypoechoic area in ultrasound images of asymptomatic carotid plaques predicts the occurrence of stroke. *J Vasc Surg*. 2013;57(3):608-609. doi:10.1016/j.jvs.2012.09.045
168. Shen Y-T, Chen L, Yue W-W, Xu H-X. Artificial intelligence in ultrasound. *Eur J Radiol*. 2021;139:109717. doi:10.1016/j.ejrad.2021.109717
169. Boyd C, Brown G, Kleinig T, et al. Machine Learning Quantitation of Cardiovascular and Cerebrovascular Disease: A Systematic Review of Clinical Applications. *Diagnostics (Basel, Switzerland)*. 2021;11(3):551. doi:10.3390/diagnostics11030551
170. Biswas M, Saba L, Chakrabartty S, et al. Two-stage artificial intelligence model for jointly measurement of atherosclerotic wall thickness and plaque burden in carotid ultrasound: A screening tool for cardiovascular/stroke risk assessment. *Comput Biol Med*. 2020;123:103847. doi:10.1016/j.combiomed.2020.103847
171. Saba L, Sanagala SS, Gupta SK, et al. Ultrasound-based internal carotid artery plaque characterization using deep learning paradigm on a supercomputer: a cardiovascular

disease/stroke risk assessment system. *Int J Cardiovasc Imaging*. 2021;37(5):1511-1528.

doi:10.1007/s10554-020-02124-9

172. Biswas M, Kuppili V, Araki T, et al. Deep learning strategy for accurate carotid intima-media thickness measurement: An ultrasound study on Japanese diabetic cohort. *Comput Biol Med*. 2018;98:100-117. doi:10.1016/j.compbiomed.2018.05.014
173. Jain PK, Sharma N, Giannopoulos AA, Saba L, Nicolaides A, Suri JS. Hybrid deep learning segmentation models for atherosclerotic plaque in internal carotid artery B-mode ultrasound. *Comput Biol Med*. 2021;136:104721. doi:10.1016/j.compbiomed.2021.104721
174. Cheng C-A, Chiu H-W. An artificial neural network model for the evaluation of carotid artery stenting prognosis using a national-wide database. *Annu Int Conf IEEE Eng Med Biol Soc IEEE Eng Med Biol Soc Annu Int Conf*. 2017;2017:2566-2569. doi:10.1109/EMBC.2017.8037381
175. Jeon JP, Kim C, Oh B-D, Kim SJ, Kim Y-S. Prediction of persistent hemodynamic depression after carotid angioplasty and stenting using artificial neural network model. *Clin Neurol Neurosurg*. 2018;164:127-131. doi:10.1016/j.clineuro.2017.12.005
176. Saba L, Jamthikar A, Gupta D, et al. Global perspective on carotid intima-media thickness and plaque: should the current measurement guidelines be revisited? *Int Angiol*. 2019;38(6):451-465. doi:10.23736/S0392-9590.19.04267-6
177. Acharya UR, Sree SV, Mookiah MRK, et al. Computed tomography carotid wall plaque characterization using a combination of discrete wavelet transform and texture features: A pilot study. *Proc Inst Mech Eng Part H J Eng Med*. 2013;227(6):643-654. doi:10.1177/0954411913480622
178. Caetano dos Santos FL, Kolasa M, Terada M, Salenius J, Eskola H, Paci M. VASIM: an automated tool for the quantification of carotid atherosclerosis by computed tomography angiography. *Int J Cardiovasc Imaging*. 2019;35(6):1149-1159. doi:10.1007/s10554-019-01549-1

179. Hanning U, Sporns PB, Psychogios MN, et al. Imaging-based prediction of histological clot composition from admission CT imaging. *J Neurointerv Surg*. Published online January 22, 2021:neurintsurg-2020-016774. doi:10.1136/neurintsurg-2020-016774
180. Le EP V, Evans NR, Tarkin JM, et al. Contrast CT classification of asymptomatic and symptomatic carotids in stroke and transient ischaemic attack with deep learning and interpretability. *Eur Heart J*. 2020;41(Supplement_2). doi:10.1093/ehjci/ehaa946.2418
181. Lal BK, Kashyap VS, Patel JB, et al. Novel Application of Artificial Intelligence Algorithms to Develop a Predictive Model for Major Adverse Neurologic Events in Patients With Carotid Atherosclerosis. *J Vasc Surg*. 2020;72(1):e176-e177. doi:10.1016/j.jvs.2020.04.306
182. Wu J, Xin J, Yang X, et al. Deep morphology aided diagnosis network for segmentation of carotid artery vessel wall and diagnosis of carotid atherosclerosis on black-blood vessel wall MRI. *Med Phys*. 2019;46(12):5544-5561. doi:10.1002/mp.13739
183. Samber DD, Ramachandran S, Sahota A, et al. Segmentation of carotid arterial walls using neural networks. *World J Radiol*. 2020;12(1):1-9. doi:10.4329/wjr.v12.i1.1
184. Chen L, Sun J, Canton G, et al. Automated Artery Localization and Vessel Wall Segmentation using Tracklet Refinement and Polar Conversion. *IEEE access Pract Innov open Solut*. 2020;8:217603-217614. doi:10.1109/access.2020.3040616
185. Balu N, Yarnykh VL, Chu B, Wang J, Hatsukami T, Yuan C. Carotid plaque assessment using fast 3D isotropic resolution black-blood MRI. *Magn Reson Med*. 2011;65(3):627-637. doi:10.1002/mrm.22642
186. Chen L, Zhao H, Jiang H, et al. Domain adaptive and fully automated carotid artery atherosclerotic lesion detection using an artificial intelligence approach (LATTE) on 3D MRI. *Magn Reson Med*. 2021;86(3):1662-1673. doi:10.1002/mrm.28794
187. Dong Y, Pan Y, Zhao X, Li R, Yuan C, Xu W. Identifying Carotid Plaque Composition in MRI with Convolutional Neural Networks. In: *2017 IEEE International Conference on Smart Computing (SMARTCOMP)*. ; 2017:1-8. doi:10.1109/SMARTCOMP.2017.7947015

188. Zhang R, Zhang Q, Ji A, et al. Identification of high-risk carotid plaque with MRI-based radiomics and machine learning. *Eur Radiol*. 2021;31(5):3116-3126. doi:10.1007/s00330-020-07361-z
189. Wang J, Börnert P, Zhao H, et al. Simultaneous noncontrast angiography and intraplaque hemorrhage (SNAP) imaging for carotid atherosclerotic disease evaluation. *Magn Reson Med*. 2013;69(2):337-345. doi:10.1002/mrm.24254
190. Koktzoglou I, Huang R, Ong AL, Aouad PJ, Aherne EA, Edelman RR. Feasibility of a sub-3-minute imaging strategy for ungated quiescent interval slice-selective MRA of the extracranial carotid arteries using radial k-space sampling and deep learning-based image processing. *Magn Reson Med*. 2020;84(2):825-837. doi:10.1002/mrm.28179
191. Ziegler M, Alfraeus J, Bustamante M, et al. Automated segmentation of the individual branches of the carotid arteries in contrast-enhanced MR angiography using DeepMedic. *BMC Med Imaging*. 2021;21(1):38. doi:10.1186/s12880-021-00568-6
192. Tang A, Tam R, Cadrin-Chênevert A, et al. Canadian Association of Radiologists White Paper on Artificial Intelligence in Radiology. *Can Assoc Radiol J = J l'Association Can des Radiol*. 2018;69(2):120-135. doi:10.1016/j.carj.2018.02.002
193. Lambin P, Rios-Velazquez E, Leijenaar R, et al. Radiomics: extracting more information from medical images using advanced feature analysis. *Eur J Cancer*. 2012;48(4):441-446. doi:10.1016/j.ejca.2011.11.036
194. (ESR) ES of R. White paper on imaging biomarkers. *Insights Imaging*. 2010;1(2):42-45. doi:10.1007/s13244-010-0025-8
195. Neri E, Del Re M, Paiar F, et al. Radiomics and liquid biopsy in oncology: the holons of systems medicine. *Insights Imaging*. 2018;9(6):915-924. doi:10.1007/s13244-018-0657-7
196. Doi K. Computer-aided diagnosis in medical imaging: historical review, current status and future potential. *Comput Med Imaging Graph*. 2007;31(4-5):198-211. doi:10.1016/j.compmedimag.2007.02.002

197. Micheel CM, Nass SJ, Omenn GS, eds. *Committee on the Review of Omics-Based Tests for Predicting Patient Outcomes in Clinical Trials.*; 2012. doi:10.17226/13297
198. Kumar V, Gu Y, Basu S, et al. Radiomics: the process and the challenges. *Magn Reson Imaging.* 2012;30(9):1234-1248. doi:10.1016/j.mri.2012.06.010
199. Aerts HJWL. The Potential of Radiomic-Based Phenotyping in Precision Medicine: A Review. *JAMA Oncol.* 2016;2(12):1636-1642. doi:10.1001/jamaoncol.2016.2631
200. Gillies RJ, Kinahan PE, Hricak H. Radiomics: Images Are More than Pictures, They Are Data. *Radiology.* 2016;278(2):563-577. doi:10.1148/radiol.2015151169
201. Yip SSF, Aerts HJWL. Applications and limitations of radiomics. *Phys Med Biol.* 2016;61(13):R150-R166. doi:10.1088/0031-9155/61/13/R150
202. Ambale-Venkatesh B, Yang X, Wu CO, et al. Cardiovascular Event Prediction by Machine Learning: The Multi-Ethnic Study of Atherosclerosis. *Circ Res.* 2017;121(9):1092-1101. doi:10.1161/CIRCRESAHA.117.311312
203. Han D, Kolli KK, Al'Aref SJ, et al. Machine Learning Framework to Identify Individuals at Risk of Rapid Progression of Coronary Atherosclerosis: From the PARADIGM Registry. *J Am Heart Assoc.* 2020;9(5):e013958. doi:10.1161/JAHA.119.013958
204. Hu X, Reaven PD, Saremi A, et al. Machine learning to predict rapid progression of carotid atherosclerosis in patients with impaired glucose tolerance. *EURASIP J Bioinforma Syst Biol.* 2016;2016(1):14. doi:10.1186/s13637-016-0049-6
205. Motwani M, Dey D, Berman DS, et al. Machine learning for prediction of all-cause mortality in patients with suspected coronary artery disease: a 5-year multicentre prospective registry analysis. *Eur Heart J.* 2017;38(7):500-507. doi:10.1093/eurheartj/ehw188
206. Quesada JA, Lopez-Pineda A, Gil-Guillén VF, et al. Machine learning to predict cardiovascular risk. *Int J Clin Pract.* 2019;73(10):e13389. doi:10.1111/ijcp.13389
207. Groenendyk JW, Mehta NN. Applying the ordinal model of atherosclerosis to imaging science: a brief review. *Open Hear.* 2018;5(2):e000861. doi:10.1136/openhrt-2018-000861

208. Terrada O, Cherradi B, Raihani A, Bouattane O. A novel medical diagnosis support system for predicting patients with atherosclerosis diseases. *Informatics Med Unlocked*. 2020;21:100483. doi:<https://doi.org/10.1016/j.imu.2020.100483>
209. van Rosendael AR, Maliakal G, Kolli KK, et al. Maximization of the usage of coronary CTA derived plaque information using a machine learning based algorithm to improve risk stratification; insights from the CONFIRM registry. *J Cardiovasc Comput Tomogr*. 2018;12(3):204-209. doi:[10.1016/j.jcct.2018.04.011](https://doi.org/10.1016/j.jcct.2018.04.011)
210. Weng SF, Reys J, Kai J, Garibaldi JM, Qureshi N. Can machine-learning improve cardiovascular risk prediction using routine clinical data? *PLoS One*. 2017;12(4):e0174944. doi:[10.1371/journal.pone.0174944](https://doi.org/10.1371/journal.pone.0174944)
211. Cires-Drouet RS, Mozafarian M, Ali A, Sikdar S, Lal BK. Imaging of high-risk carotid plaques: ultrasound. *Semin Vasc Surg*. 2017;30(1):44-53. doi:[10.1053/j.semvascsurg.2017.04.010](https://doi.org/10.1053/j.semvascsurg.2017.04.010)
212. Rafailidis V, Huang DY, Yusuf GT, Sidhu PS. General principles and overview of vascular contrast-enhanced ultrasonography. *Ultrason (Seoul, Korea)*. 2020;39(1):22-42. doi:[10.14366/usg.19022](https://doi.org/10.14366/usg.19022)
213. Wannarong T, Parraga G, Buchanan D, et al. Progression of carotid plaque volume predicts cardiovascular events. *Stroke*. 2013;44(7):1859-1865. doi:[10.1161/STROKEAHA.113.001461](https://doi.org/10.1161/STROKEAHA.113.001461)
214. Kuk M, Wannarong T, Beletsky V, Parraga G, Fenster A, Spence JD. Volume of carotid artery ulceration as a predictor of cardiovascular events. *Stroke*. 2014;45(5):1437-1441. doi:[10.1161/STROKEAHA.114.005163](https://doi.org/10.1161/STROKEAHA.114.005163)
215. Madani A, Beletsky V, Tamayo A, Munoz C, Spence JD. High-risk asymptomatic carotid stenosis: ulceration on 3D ultrasound vs TCD microemboli. *Neurology*. 2011;77(8):744-750. doi:[10.1212/WNL.0b013e31822b0090](https://doi.org/10.1212/WNL.0b013e31822b0090)
216. Nies KPH, Smits LJM, Kassem M, Nederkoorn PJ, van Oostenbrugge RJ, Kooi ME.

Emerging Role of Carotid MRI for Personalized Ischemic Stroke Risk Prediction in Patients With Carotid Artery Stenosis. *Front Neurol.* 2021;12:718438.

doi:10.3389/fneur.2021.718438

217. Kassem M, Florea A, Mottaghy FM, van Oostenbrugge R, Kooi ME. Magnetic resonance imaging of carotid plaques: current status and clinical perspectives. *Ann Transl Med.* 2020;8(19):1266. doi:10.21037/atm-2020-cass-16
218. Baradaran H, Myneni PK, Patel P, et al. Association Between Carotid Artery Perivascular Fat Density and Cerebrovascular Ischemic Events. *J Am Heart Assoc.* 2018;7(24):e010383. doi:10.1161/JAHA.118.010383
219. Baradaran H, Eisenmenger LB, Hinckley PJ, et al. Optimal Carotid Plaque Features on Computed Tomography Angiography Associated With Ischemic Stroke. *J Am Heart Assoc.* 2021;10(5):e019462. doi:10.1161/JAHA.120.019462
220. Sun J, Song Y, Chen H, et al. Adventitial perfusion and intraplaque hemorrhage: A dynamic contrast-enhanced MRI study in the carotid artery. *Stroke.* 2013;44(4):1031-1036. doi:10.1161/STROKEAHA.111.000435
221. Paraskevas KI, Spence JD, Veith FJ, Nicolaides AN. Identifying which patients with asymptomatic carotid stenosis could benefit from intervention. *Stroke.* 2014;45(12):3720-3724. doi:10.1161/STROKEAHA.114.006912
222. Naylor AR, Ricco J-B, de Borst GJ, et al. Editor's Choice - Management of Atherosclerotic Carotid and Vertebral Artery Disease: 2017 Clinical Practice Guidelines of the European Society for Vascular Surgery (ESVS). *Eur J Vasc Endovasc Surg Off J Eur Soc Vasc Surg.* 2018;55(1):3-81. doi:10.1016/j.ejvs.2017.06.021
223. Saba L, Mossa-Basha M, Abbott A, et al. Multinational Survey of Current Practice from Imaging to Treatment of Atherosclerotic Carotid Stenosis. *Cerebrovasc Dis.* 2021;50(1):108-120. doi:10.1159/000512181
224. Paraskevas KI, Mikhailidis DP, Baradaran H, et al. Management of Patients with

Asymptomatic Carotid Stenosis May Need to Be Individualized: A Multidisciplinary Call for Action. *J stroke*. 2021;23(2):202-212. doi:10.5853/jos.2020.04273

Figure legends

Figure 1. Automated measurement of Vessel Wall volume.

A. Automated segmentation (yellow line) was very accurate compared to manual segmentation by experts (red line). Dice-similarity-coefficient (DSC) was $93.2 \pm 3.0\%$ for the Medial-Arterial Boundary in the common carotid artery and $91.9 \pm 5.0\%$ in the bifurcation. DSC for the Lumen-Intima Boundary was $89.5 \pm 6.7\%$ and $89.3 \pm 6.8\%$ for the Common Carotid Artery and the bifurcation respectively. Automated segmentation took less than one second for each side.

B. Relationships of the automated and manual VWV measurements for $n=302$ 3DUS images in the CAIN dataset. (a) Linear correlation ($r = 0.876$, $p = 0.0001$), and (b) Bland-Altman plot of the two

sets of VWV measurements. The solid red line and the dash red lines represent the bias (-3.6 mm^3) and $\text{mean} \pm 1.96 \text{ SD}$, respectively.

(Reproduced by permission of IEEE from: Zhou R, Guo F, Azarpazhooh MR, Spence JD, Ukwatta E, Ding M and Fenster A. A Voxel-Based Fully Convolution Network and Continuous Max-Flow for Carotid Vessel-Wall-Volume Segmentation From 3D Ultrasound Images. *IEEE Trans Med Imaging*. 2020;39:2844-2855.)

Figure 2. Carotid artery dissection (panel a, b) in a 49-year-old female patient. The CTA shows the filiform lumen in the right ICA (a) that is confirmed by the MR (b). Infective pseudo-aneurysm in 63-year-old male patient (panel c, d). The CTA shows the contrast material due to into the pseudoaneurysm (white open arrows, panel c) and the volume rendered image (d) confirms the spatial relationship.

Figure 3. Metabolic activity within atherosclerotic carotid plaque, imaged with [^{18}F]-fluorodeoxyglucose (^{18}F FDG) hybrid PET /CT correlates with ex-vivo macrophage-specific CD68 CT angiography (axial plane) fused with [^{18}F]-fluorodeoxyglucose PET in a patient with a symptomatic right internal carotid artery plaque (arrow). From the fused PET/CT images, there are small regions of calcification with a narrowing of the right internal carotid artery. The tissue to blood ratio for maximum ^{18}F FDG uptake was 4.7. Following excision and advanced immunohistology, there is strong evidence for extensive CD68 staining (rust-stained regions), a marker of macrophage expression and direct inflammatory burden.

(Reproduced by permission of Elsevier from: Cocker MS, Spence JD, Hammond R, et al. [^{18}F]-Fluorodeoxyglucose PET/CT imaging as a marker of carotid plaque inflammation: Comparison to immunohistology and relationship to acuity of events. *International Journal of Cardiology*. 2018;271:378-386.)

Figure 4: A) laser-angiography showing an acutely disrupted plaque with red blood cell rich intraluminal thrombus resulting in critical stenosis; b) IVUS images with doppler mode of a symptomatic calcified plaque causing severe irregular stenosis; c) OCT images showing stent apposition in a carotid artery.

Figure 5. Venn diagram illustrating the hierarchy of the artificial intelligence fields

Figure 6. Basic representation of an artificial neural network with neurons similar to those within a brain. The left layer of the neural network is called the input layer and contains neurons that encode the values of the input pixels. The right most layer is called the output layer, which contains the output neurons. The middle contains the “n” number of hidden layers, which perform mathematical transformations of the data.

Tables

Table 1: Main imaging methods for carotid arteries

	Atherosclerosis is Vulnerable plaque	Accuracy	Sensitivity	Burden	Availability	Standardization
Ultrasound	++ +-	+	+++	-	+++	+-
CT angiography	++ --	++	++	++	+-	++
Magnetic Resonance	+++ ++	++	+++	-	--	+-

Positron emission tomography	+++ +++	+	+++	+	---	+ -
-------------------------------------	------------	---	-----	---	-----	-----

Table 2. (Duplex-)Sonographic criteria for grading internal carotid artery stenosis and markers of carotid plaque vulnerability

Sonographic marker	Classification / Feature of plaque vulnerability
Grading of internal carotid artery stenosis based on Duplex ultrasound	Degree of stenosis as defined by NASCET [1] <ul style="list-style-type: none"> - < 50%: plaque on B-mode, aliasing on color duplex image, PSV < 200cm/s - 50-69%: PSV 200-300cm/s, EDV <100cm/s, PSV ratio (ICA/CCA) ≥ 2 - $\geq 70\%$: PSV > 300cm/s, EDV > 100cm/s, PSV ratio (ICA/CCA) ≥ 4 Progression of degree of stenosis (>20%) [5]
Echogenicity on B-mode ultrasound	hypoechogenic (echolucent) plaque (type 1 or type 2) [8] «Grey scale median (GSM)»: GSM < 15 (hypoechogenic) [9] Increased juxta-luminal hypoechogenic (black) area (> 6 mm ²) [10] Heterogenic echotexture [11, 12]
Plaque burden on B-mode ultrasound including 3D-ultrasound	Large plaque area (> 40mm ²) [9] / total plaque area [13, 14] Large plaque volume / total plaque volume (3D-Ultrasound) [12, 13]
Carotid plaque surface on Duplex-	Plaque surface irregularities (<1-2 mm) [11]

ultrasound and CEUS	Plaque ulceration (>1-2mm) [11]
Carotid intraplaque neovascularization (IPN) on CEUS	<p>Increased IPN on semi-quantitative measurement [18, 22]:</p> <ul style="list-style-type: none"> • grade 1: no vascularization • grade 2: limited or moderate vascularization • grade 3: extensive vascularization <p>High IPN on semiautomatic quantitative measurement: e.g. large relative perfused area [24-26]</p>

Peak systolic flow velocity (PSV), end-diastolic flow velocity (EDV)

Table 3

	Imaging features	Supporting evidence	Limitations	General limitations
IPH	<p>Directly: attenuation values ≤ 25</p> <p>Indirectly: calcified rim and soft internal plaque</p>	Moderate supporting evidence	Similar HU attenuation values between soft plaque components	<ul style="list-style-type: none"> •Radiation dose delivered to the patients •Potential side effect •The limit tissue contrast between soft plaque components •Overestimates the degree of the stenosis due to calcium deposits
LNRC	Presence of soft plaque components	Conflicting supporting evidence	Artifact related to halo-effect and edge-blur	
Plaque inflammation	Presence of contrast plaque enhancement	Weak supporting evidence		

Neovascularization	Presence of contrast plaque enhancement	Moderate supporting evidence		
Plaque surface Morphology	Alterations of the luminal surface on the luminal profile of the plaque	Strong supporting evidence	Presence of a halo or edge blur may hinder detection of smaller ulcerations.	
Plaque Volume and composition	Size of the carotid plaque with its subcomponents	Strong supporting evidence	Limit tissue contrast attenuation in some plaque subcomponents	
Calcifications	Size and morphology of calcium deposits	Strong supporting evidence		

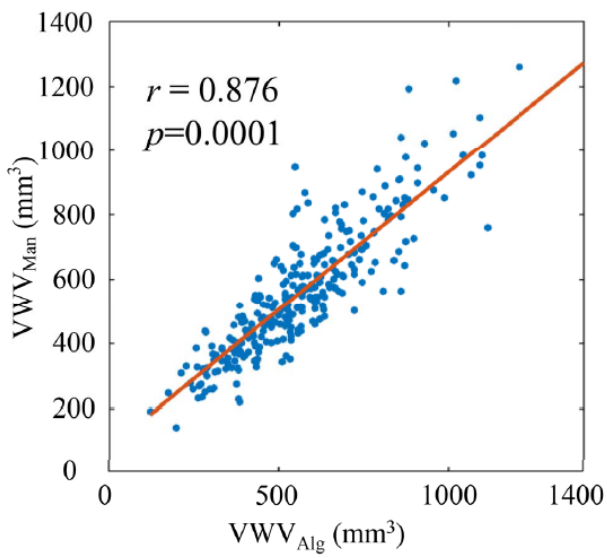
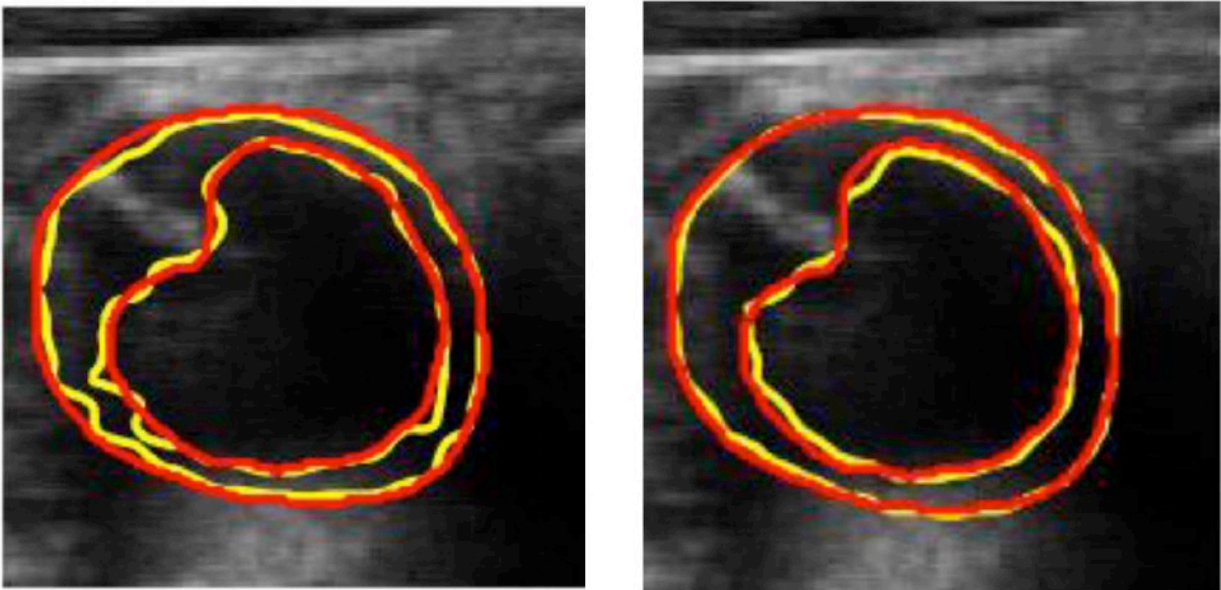
Table 4

Condition	Comments
Congenital	Agensis, aplasia or hypoplasia of ICA
Inflammatory & infectious conditions	Carotidynia Giant cell arteritis Takayasu arteritis Post-radiation arteritis
Carotid dissection	Traumatic or spontaneous Consider underlying condition with spontaneous (e.g. FMD)
Carotid web & floating thrombus	Associated with increased stroke risk

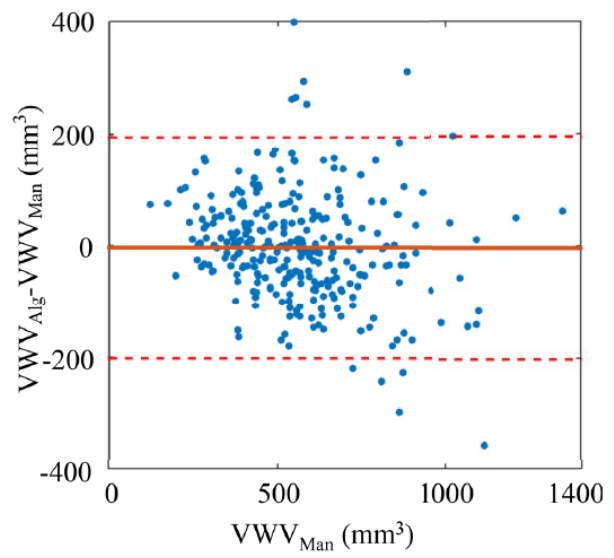
Figures

Figure 1

Figure 1



(a)



(b)

Figure 1: Automated measurement of Vessel Wall volume.

A. Automated segmentation (yellow line) was very accurate compared to manual segmentation by experts (red line). Dice-similarity-coefficient (DSC) was $93.2\pm 3.0\%$ for the Medial-Arterial Boundary in the common carotid artery and $91.9\pm 5.0\%$ in the bifurcation. DSC for the Lumen-Intima Boundary was $89.5\pm 6.7\%$ and $89.3\pm 6.8\%$ for the Common Carotid Artery and the bifurcation respectively. Automated segmentation took less than one second for each side.

B. Relationships of the automated and manual VWV measurements for $n=302$ 3DUS images in the CAIN dataset. (a) Linear correlation ($r = 0.876$, $p = 0.0001$), and (b) Bland-Altman plot of the two sets of VWV measurements. The solid red line and the dash red lines represent the bias (-3.6 mm^3) and $\text{mean}\pm 1.96 \text{ SD}$, respectively.

(Reproduced by permission of IEEE from: Zhou R, Guo F, Azarpazhooh MR, Spence JD, Ukwatta E, Ding M and Fenster A. A Voxel-Based Fully Convolution Network and Continuous Max-Flow for Carotid Vessel-Wall-Volume Segmentation From 3D Ultrasound Images. *IEEE Trans Med Imaging*. 2020;39:2844-2855.)

Figure 2

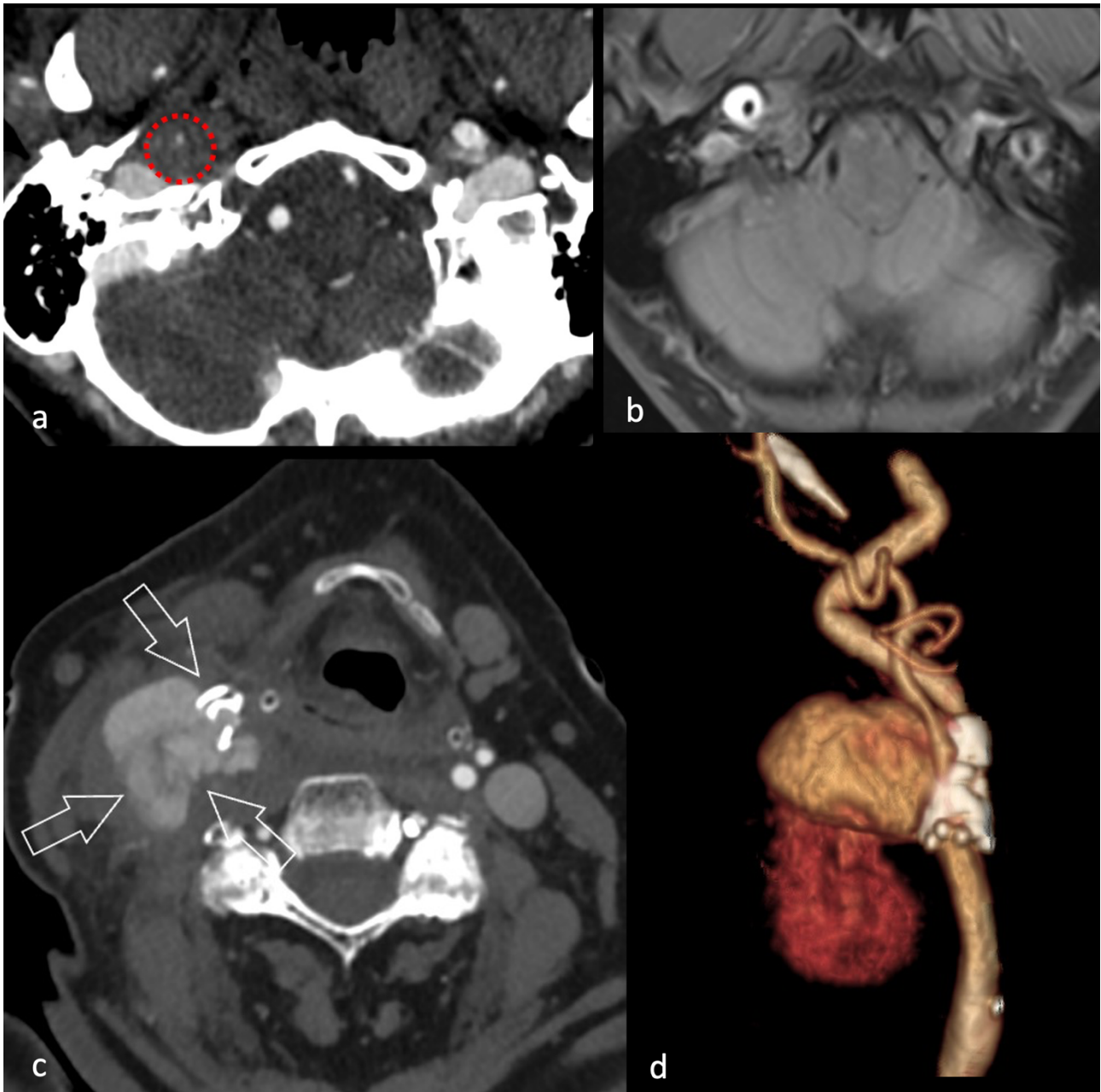


Figure 2. Carotid artery dissection (panel a, b) in a 49-year-old female patient. The CTA shows the filiform lumen in the right ICA (a) that is confirmed by the MR (b). Infective pseudo-aneurysm in 63-year-old male patient (panel c, d). The CTA shows the contrast material due to into the

pseudoaneurysm (white open arrows, panel c) and the volume rendered image (d) confirms the spatial relationship.

Figure 3

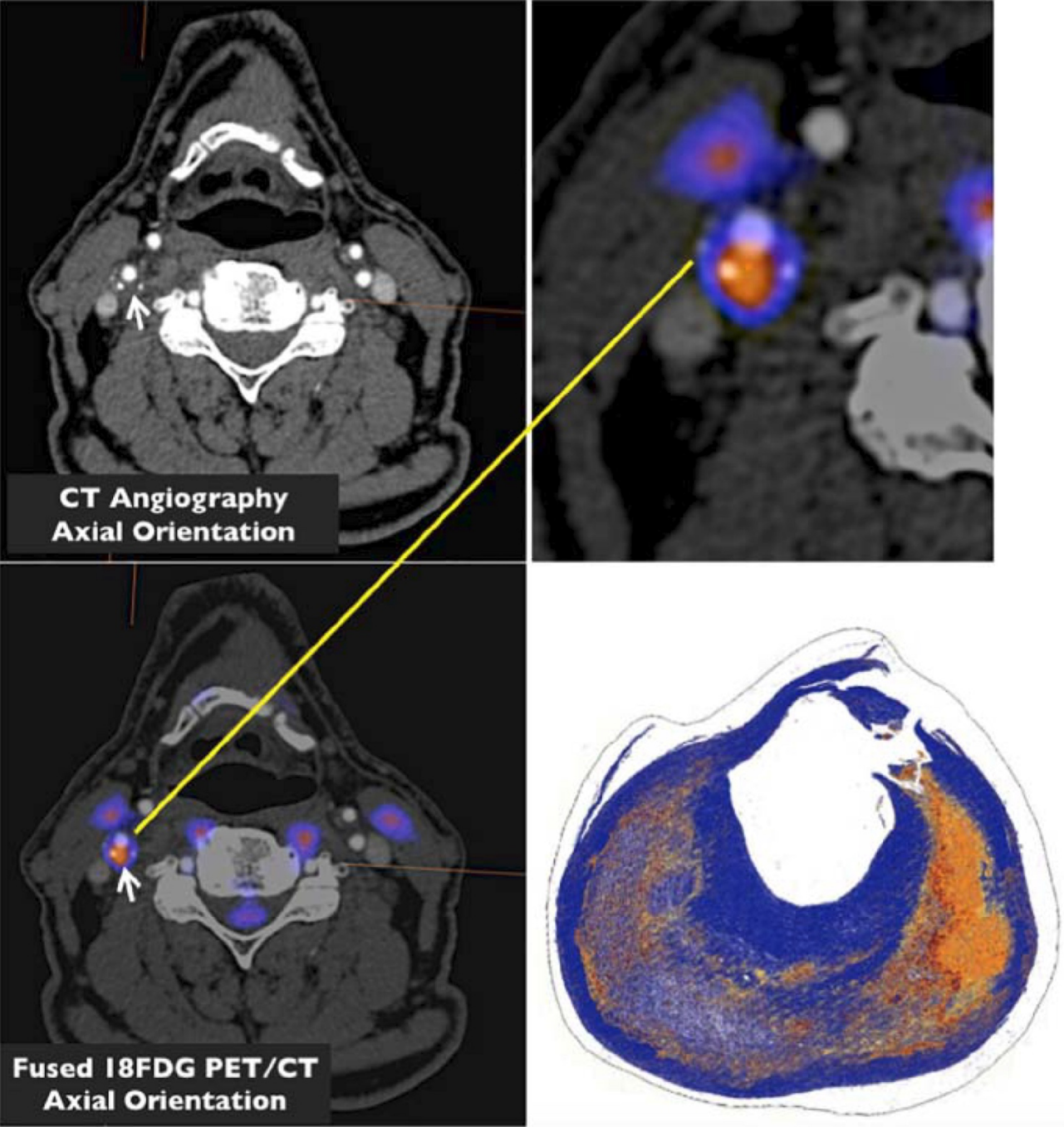


Figure 3. Metabolic activity within atherosclerotic carotid plaque, imaged with [18F]-fluorodeoxyglucose (18FDG) hybrid PET /CT correlates with ex-vivo macrophage-specific CD68 CT angiography (axial plane) fused with [18F]-fluorodeoxyglucose PET in a patient with a symptomatic right internal carotid artery plaque (arrow). From the fused PET/CT images, there are small regions of calcification with a narrowing of the right internal carotid artery. The tissue to blood ratio for maximum 18FDG uptake was 4.7. Following excision and advanced immunohistology, there is strong evidence for extensive CD68 staining (rust-stained regions), a marker of macrophage expression and direct inflammatory burden.

(Reproduced by permission of Elsevier from: Cocker MS, Spence JD, Hammond R, et al. [18F]-Fluorodeoxyglucose PET/CT imaging as a marker of carotid plaque inflammation: Comparison to immunohistology and relationship to acuity of events. *International Journal of Cardiology*. 2018;271:378-386.)

Figure 4

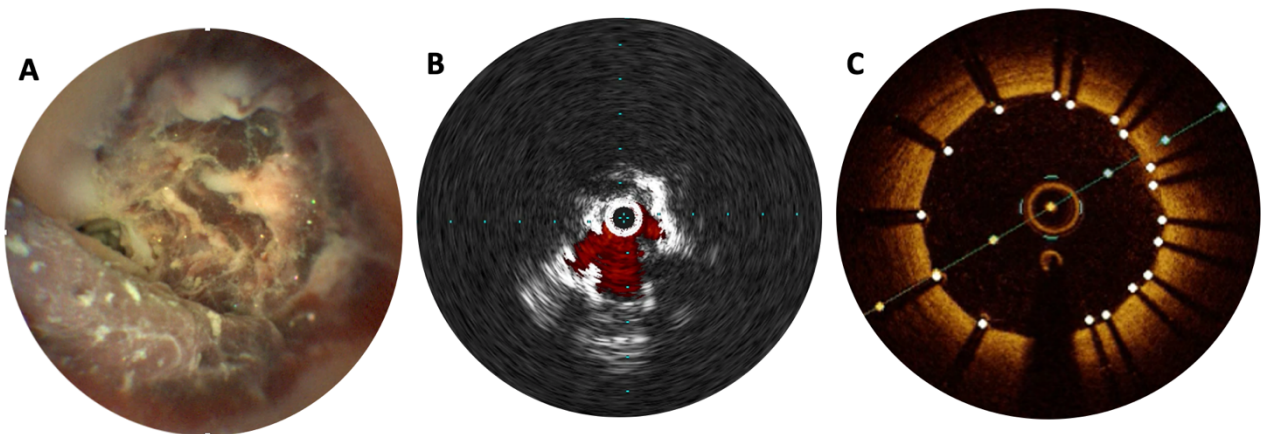


Figure 4: A) laser-angiography showing an acutely disrupted plaque with red blood cell rich intraluminal thrombus resulting in critical stenosis; b) IVUS images with doppler mode of a symptomatic calcified plaque causing severe irregular stenosis; c) OCT images showing stent apposition in a carotid artery.

Figure 5

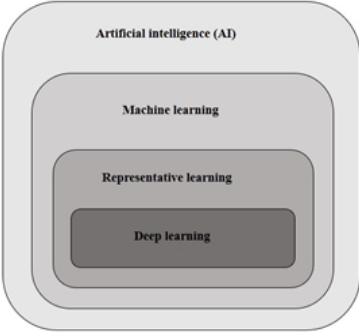


Figure 5. Venn diagram illustrating the hierarchy of the artificial intelligence fields

Figure 6

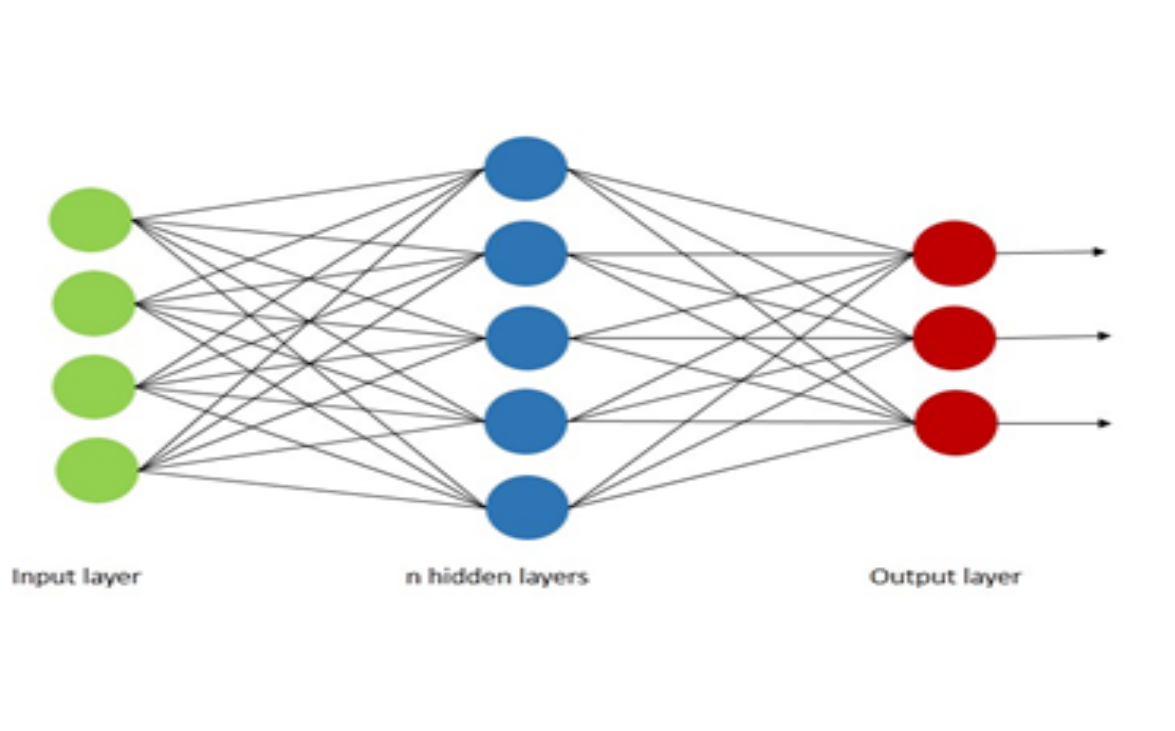


Figure 6. Basic representation of an artificial neural network with neurons similar to those within a brain. The left layer of the neural network is called the input layer and contains neurons that encode the values of the input pixels. The right most layer is called the output layer, which contains the output neurons. The middle contains the “n” number of hidden layers, which perform mathematical transformations of the data.

